Alma Mater Studiorum - Università di Bologna

SCUOLA DI SCIENZE

Dipartimento di Chimica Industriale "Toso Montanari"

Corso di Laurea Magistrale in

Chimica Industriale

Classe LM-71 - Scienze e Tecnologie della Chimica Industriale

Synthesis, Characterization and Catalytic Performances of Ruthenium-based Catalysts for the Acceptorless Dehydrogenative Coupling of Butanol

Tesi di laurea sperimentale

CANDIDATO

Andrea Bernardi

RELATORE

Prof. Daniele Nanni

CORRELATORI

Dott. Simon Desset

Dott. Guillaume Raffa

Sessione III

Anno Accademico 2013-2014

Abstract

A growing interest towards new sources of energy has led in recent years to the development of a new generation of catalysts for alcohol dehydrogenative coupling (ADC). This green, atom-efficient reaction is capable of turning alcohol derivatives into higher value and chemically more attractive ester molecules, and it finds interesting applications in the transformation of the large variety of products deriving from biomass.

In the present work, a new series of ruthenium-PNP pincer complexes are investigated for the transformation of 1-butanol, one of the most challenging substrates for this type of reactions, into butyl butyrate, a short-chain symmetrical ester widely used in flavor industries.

Since the reaction kinetics depends on hydrogen diffusion, the study aimed at identifying proper reactor type and right catalyst concentration to avoid mass transfer interferences and to get dependable data.

A comparison between catalytic activities and productivities has been made to establish the role of the different ligands bonded both to the PNP binder and to the ruthenium metal center, and hence to find the best catalyst for this type of reaction.

Summary

1. ***Introduction***
    1.1. Renewable and non-renewable energy
        1.1.1. Biomass
        1.1.2. Biofuels vs fossil fuels
        1.1.3. First and second generation biomass
        1.1.4. Biofuels and bioproducts: ethanol and butanol
    1.2. Alcohol dehydrogenative coupling
        1.2.1. Dehydrogenative activation of alcohols
        1.2.2. Acceptorless alcohol dehydrogenation
        1.2.3. Acceptorless dehydrogenative coupling of primary alcohols
2. ***Purpose of the project***
    2.1. New catalysts
    2.2. Hydrogen transfer limitations
3. ***Experimental part***
    3.1. Materials
    3.2. Analytical instruments and methods
    3.3. Standard procedure for catalytic test
    3.4. Sampling method
    3.5. Complex synthesis
4. ***Results and discussions***
    4.1. Reactor type
    4.2. Catalyst structure-reactivity
    4.3. Catalyst deactivation/reactivation
5. ***Conclusions***

1. Introduction

1.1. Renewable and non-renewable energy

Despite the growing global awareness towards renewable energy sources, fossil fuels still remain the main energy fount of the planet. In 2012, coal, petroleum, and natural gas accounted for 78.4 % of the global energy consumption[1].

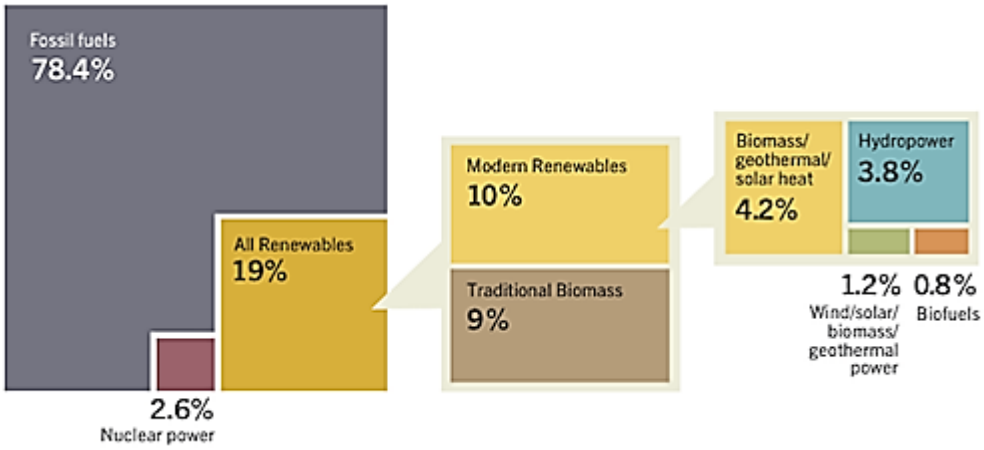

Figure 1. Global sources of energy[1]

In addition to be the primary energy source, fossil raw materials are also transformed into a large variety of chemicals, such as plastic polymers, asphalt, fertilizers, etc., which have become increasingly important in every day's life. The intensive and disparate use of this non-renewable raw materials always leaves in the background concerns about its exhaustion in short or middle-term, as well as all the well-known problems related to the use of oil, i.e. greenhouse gas emissions (CO, CO_2, NO_x, SO_2), difficulties in the transportation and extraction (since 2010 we can count at least eight oil spills around the world for a total amount of over 500,000 tons of crude oil released into the environment[2]), unequal distribution of resources all over the world (that leads to socioeconomic conflicts). In this context, exploring alternative renewable, environmentally friendly sources of energy, fuels, and chemicals has become a fundamental issue in recent years.

Biomass represents the only abundant, alternative source of organic carbon that can allow for a wide variety of chemical transformations. In fact, biomass molecules are highly functionalized (with mainly hydroxyl, carbonyl, and carboxylic groups), which makes them more suitable than crude oil to be used as starting materials for the production of high added-value chemicals.

1.1.1. Biomass

A key feature is the wide availability of biomass and its abundance in every different area of the planet; this would limit the dependence on imported raw materials and minimize fluctuations in market prices, leading, perhaps, to an energy self-sufficiency that would restrict socio-economic conflicts.

Indeed, among the various origin of biomass we can identify:

- agricultural crops (corn, sugarcane, soybean, molasses and several others, depending on the geographic area);
- specific crops (often aimed at the simple production of wood to be treated);
- secondary products, such as waste from food industries or farms;
- forest biomass (derived by pruning or deforestation);
- algae and microorganisms from bioreactors;
- organic fraction from municipal waste collection.

Although the use of biomass is varied (from fuels, lubricants, solvents, through precursors of polymers and plastics, surfactants, detergents and fine chemicals, up to basic chemicals and fillers), it can be divided into two major classes:

1. products that replace existing molecules of petrochemical origin in production processes already established (biofuels);
2. bioproducts, which require the integration into existing production processes or the creation of new ones.

We can hence say that, in general, the biomass has three basic uses, all for the purpose of energy recovery: biofuel production, manufacturing of bio-based products, and direct combustion.

The intrinsic calorific value of biomass makes not convenient any disposal in landfills, but rather the *in situ* combustion, which was the most common, simplest use in the past, although the one with the highest environmental impact (release of CO_2 from combustion and of NO_x resulting from the nitrogen fertilizers used in the growth phase).

The possibility of obtaining clean energy by processing biomass has recently been rediscovered by global institutions, which have started incentive policies and funding for the promotion of low-emission industries[3].

Figure 2. Targets for bio-based industries [4]

1.1.2. Biofuels vs fossil fuels

Industrial production of biofuels began in 1916 with the development of ABE (Acetone-Butanol-Ethanol) fermentation techniques by the use of the bacterium *Clostridia acetobutylicum*, first isolated by Weizman[5][6]. This process was used up to the 1920th exclusively for producing acetone (and then cordite for firearms[7]), which however was found to be not the major product (since each mole of acetone is accompanied by formation of two moles of butanol). This procedure was carried out industrially throughout the United States during the first half of the last century, but it was discontinued in the early 1960s due to unfavorable economic conditions brought about by competition with the petrochemical industry[8]. However, since the discovery of this type of processes, a new generation of biofuels was born, with some better features than traditional fossil fuels, but also with some more limitation.

Advantages:

- carbon neutral: when burned, a biofuel produces less carbon emission and, in particular, an amount comparable to the carbon absorbed by photosynthesis by the next harvest;

- source of materials: instead of oil, biofuels can be produced from a wide range of materials (corns, molasses, sugarcanes, soybeans, ...);

- renewability: sustainable production of raw materials;

- less content of molecular oxygen: reduced release of pollutants in the air;

- costs: significantly less expensive than gasoline or other fossil fuels, especially in the view of an increasing demand against a lower availability of non-renewable resources;

- socio-economic impact: a local production decreases dependence on foreign fuel sources, and increases local employment (creation of new manufacturing plants) and agricultural development and production.

Disadvantages:

- energy output: energy content in biomass is only half of that of crude oil on a weight bases (greater quantities are required in order to produce the same energy level);

- carbon emissions: to make new areas available for cultivation of raw materials for biomass, and hence for production of biofuels, entails higher emissions of carbon oxides;

- high costs: the processes mentioned above imply a significantly higher energy consumption and a massive use of water;

- food prices and shortages: an increase in demand for products destined to the production of biofuels can lead to a decrease of the availability of the same products for the food market, with a consequent increase of prices.

1.1.3. First and second generation biomass

The great demand for products intended for the production of biomass could lead to a reduced availability of the same products for the food market, and to a consequent rise in prices. To address this problem, a new generation of biomass transformation processes has been developed in recent years, which do not use products directly competitive with agricultural market but instead includes non-edible part of plants (lignocellulosic biomass), or microalgae systems (bioreactors)[9][10].

From the production point of view, first and second generation processes rely on completely different techniques. If the processes to produce biomass of first generation have been known since the beginning of 1900, and even before (alcohol and ABE fermentation), and involve fermentation of simple sugars (monosaccharides such as glucose and disaccharides such as sucrose)[11], or easily hydrolysable sugar polymers (starch), for the production of second generation biomass (excluding microalgae systems), non-hydrolysable carbohydrate polymers are used, such as cellulose, together with hemicellulose, and lignin.

Cellulose is the world's most abundant polymer[12]. It is the structural component of plant cell walls, providing rigidity and mechanical resistance to the plant.

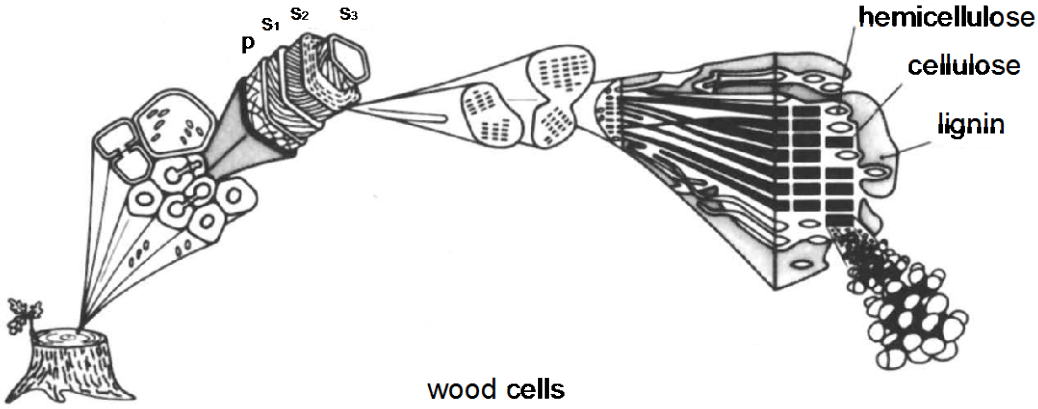

p, primary walls; s_1, s_2, s_3, outer, inner and terminal secondary walls, respectively.

Figure 3. Lignocellulose structure in woods cell.

As a biodegradable, non-petroleum-based and carbon neutral resource, it has versatile uses in biofuel production[13], pharmaceutical industries[14-15], bioelectronic devices[16], medical care[17], etc. Cellulose is a linear polymer composed by glucose units covalently linked though β (1 – 4) glycosidic bonds[18]. Its highly crystalline structure is responsible for its resistance towards hydrolysis and its difficult process.

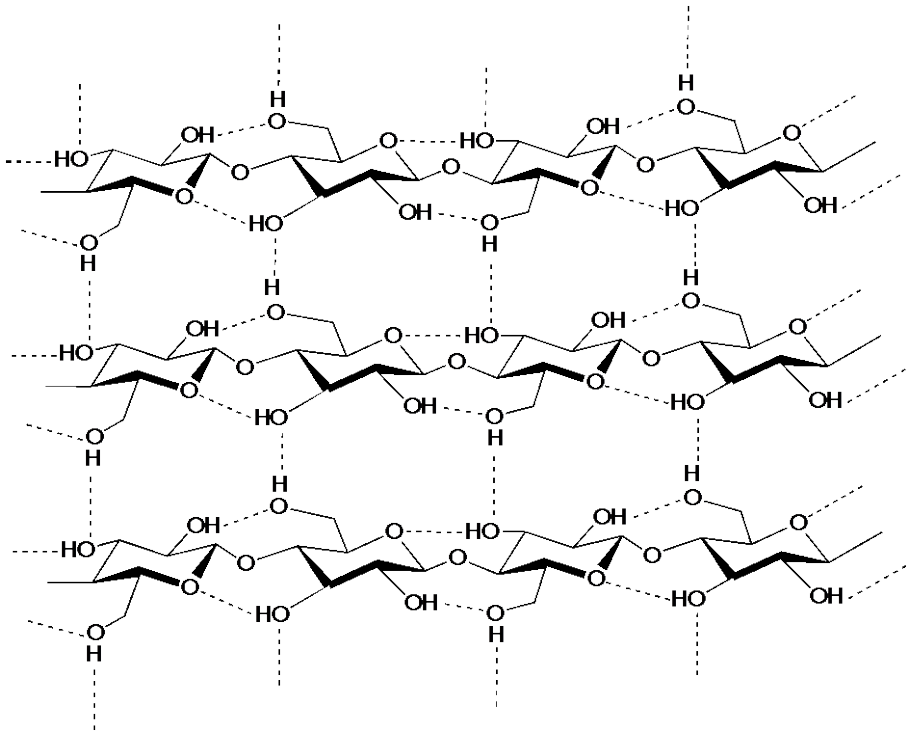

Figure 4. Structure of cellulose.

Hemicellulose is a branched polymer, composed of different C_5 and C_6 sugar monomers (glucose, xylose, mannose, galactose, etc.), which give an amorphous structure to the molecule.

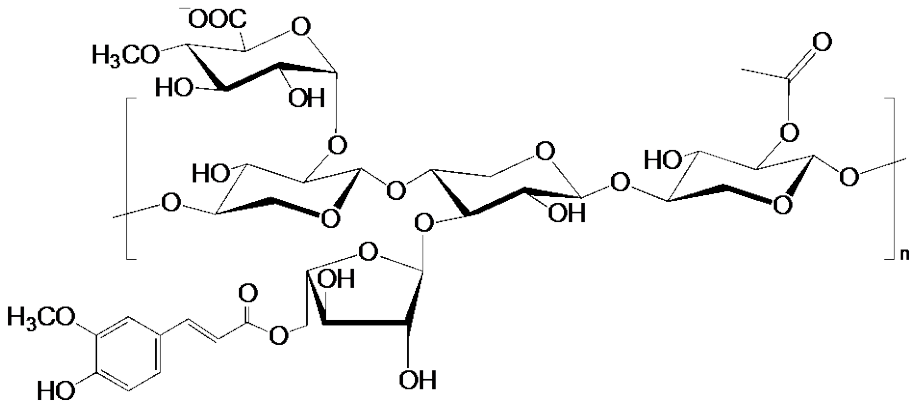

Figure 5. One possible structure of hemicelluloses.

Lignin is a three dimensional polymer made up of *p*-coumaryl, coniferyl, and sinapyl alcohols[19]. In woody biomass, lignin holds together the cellulose fibers and guarantees protection against moisture and micro-organisms. Although today it cannot be efficiently transformed into valuable product, if burned, it provides the energy required to process the

other two fractions. The typical processing of lignocellulosic biomass starts with a pretreatment of grinding and separation of the three main biopolymers. They are then depolymerized to recover the constituting monomers, C5 and C6 sugars from cellulose and hemicelluloses and phenols from lignin. These primary platform molecules are then converted into a wide range of chemicals, using single or multi-steps chemical or biochemical processes.

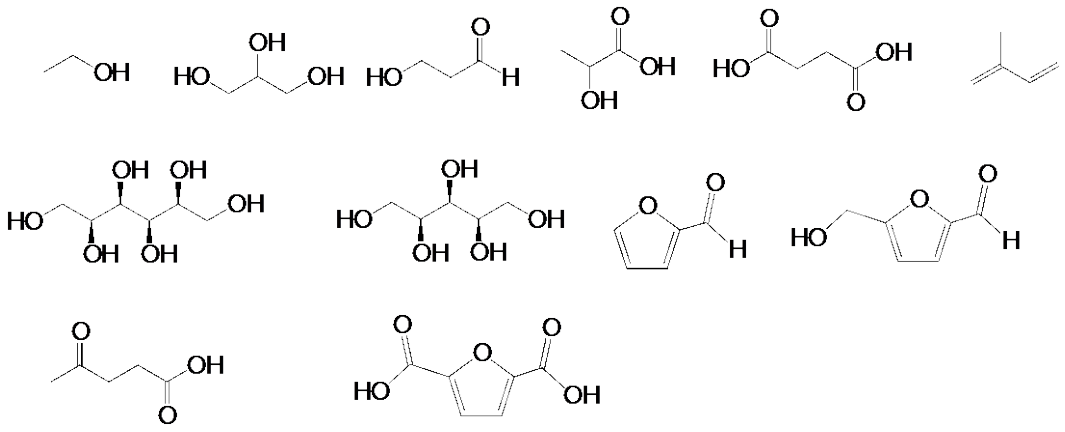

Figure 6. Structure for some top value added chemicals from biomass.

1.1.4. Biofuels and bioproducts: ethanol and butanol

As mentioned above, biomass undergoes transformations aimed at the production of two different types of products: biofuels and bio-based products, which differ either in their ability to substitute fuels in already existing processes, or to be used as "building blocks" for the development of new processes. This distinction seems to fade if we consider two short chain bioalcohols: ethanol and butanol.

Bioethanol can be produced from sugar derivatives[20] (alcohol fermentation, first generation biomass), or directly from lignocellulosics[21] (second generation biomass). Its use in place of traditional fossil fuels was discovered by Henry Ford himself, who first designed in 1941 a car made entirely of plastic materials derived from soybeans and hemp, and fueled with ethanol hemp[22]. Compared to traditional fuels, bioethanol has the advantage of reducing pollutants emissions into the atmosphere, but the disadvantage of producing a smaller amount of energy from the combustion, and to have a high volatility that makes it difficult to storage and transport.

Biobutanol can also be obtained by fermentation of first and second generation biomass[23-24], and it provides numerous advantages over ethanol. Since it has energy density, air-fuel ratio, and octane number comparable to those of gasoline (much higher than those of ethanol), it can be used in currently working cars, mixed with the same gasoline, without any modification of their systems for the formation of the air-fuel mixture. Moreover, its combustion produces neither nitrogen nor sulfur oxides (lower environmental impact). In addition, it is less corrosive and hygroscopic than ethanol, so it can be transported using the existing infrastructures[25]. Butanol, like ethanol, beside their use as biofuel, are also crucial bulk chemicals with a wide range of industrial uses (solvent, feedstock for synthesis, paint thinner, etc.).

We can hence say that these two compounds are the most versatile molecules arising from biomass. Nevertheless, it can be seen from the chemical structure of the original biopolymers (cellulose, hemicellulose and lignin), the primary platform molecules (C_5-C_6 sugars), and the expected product deriving from biomass (see Figure 6), that there is an overwhelming abundance of hydroxyl groups among all these compounds. Therefore, reactions that could transform their alcohol functionalities into something more versatile chemical functionalities would be a considerable leverage to turn biomass derived molecules into high value-added products.

1.2. Alcohol dehydrogenative coupling

1.2.1. Dehydrogenative activation of alcohols

An alcohol molecule is not a real versatile platform on its own. Its reactivity is due to the presence of two different active sites: the C-O bond and the O-H bond. Due to the electronegativity of the oxygen atom, in comparison to that of the adjacent carbon and hydrogen, those bonds can be the origin of electrophilic (carbon and hydrogen atoms) or nucleophilic (oxygen atom) behaviours. So that interesting reactions can occur, this type of molecule can be activated in two different ways, i.e. using an acid promoter or through a base. The acid leads to a protonated alcohol with an electrophilic C1-carbon and a very good leaving group, whereas the base leads to a strongly nucleophilic alkoxide.

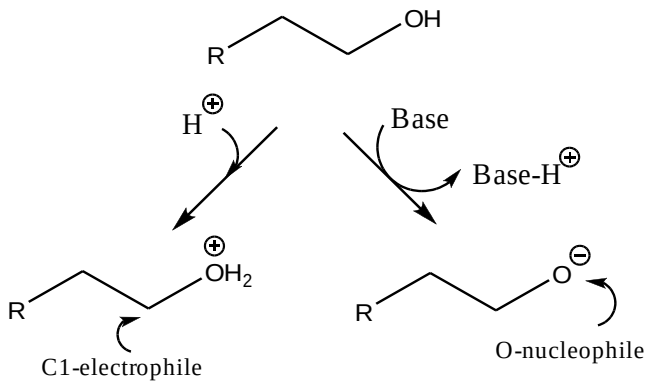

Scheme 1. General alcohol activation.

On the other hand, carbonyl compounds are much more versatile reactants, with countless uses in different types of industries. This is the main reason why selective oxidation of the alcohol functionality into carbonyl groups has been thoroughly studied for decades [26-27], using both homogeneous and heterogeneous catalytic systems. For example, the catalytic transformation of alcohols to aldehydes or ketones (depending on the starting molecule) can be attained with molecular oxygen and water as by-product; nevertheless, the use of large amounts of O_2 can yield to overoxidation of the carbonyl compound into carbon dioxide and/or carboxylic acid.

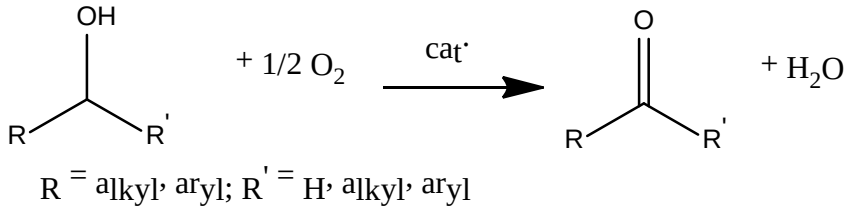

Scheme 2. General oxidation of alcohols.

In recent years, chemists have studied and developed different strategies to replace waste generating (or somewhat inefficient) synthetic routes by others in agreement with the principles of Green Chemistry. In this respect, a very elegant alternative methodology for oxidation of alcohols is the acceptorless alcohol dehydrogenation (AAD), that turns alcohols into the corresponding aldehydes or ketones with concomitant formation of molecular hydrogen.

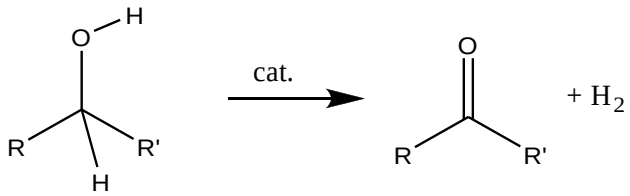

R= alkyl, aryl; R'= H, alkyl, aryl

Scheme 3. Catalytic oxidation of alcohols.

This type of transformation is preferable to the above-mentioned aerobic oxidation . On one hand, it avoids problems related to overoxidation and, on the other hand, it is best in terms of atom economy, with the additional benefit of generation of molecular hydrogen, which can be used for energy production/storage or as a reductant in other synthetically useful transformations.

Moreover, the eventual carbonyl compound can be further transformed *in situ* into a large variety of organic compounds, such as esters, carboxylates, amines, amides, or heavier alcohols. For example, the acceptorless dehydrogenation of a primary alcohol leads to an aldehyde, which can be attacked by a nucleophile to yield an addition compound (e.g. hemiacetal, hemiaminal, or hydrate). This intermediate can be further dehydrogenated to give a carboxylic acid derivatives, such as esters or amides. Alternatively, it can be dehydrated to an unsaturated compound that can be further dehydrogenated to obtain an ultimate substitution product (Scheme 4). This borrowing hydrogen mechanism is a way to obtain amines from alcohols[28-29].

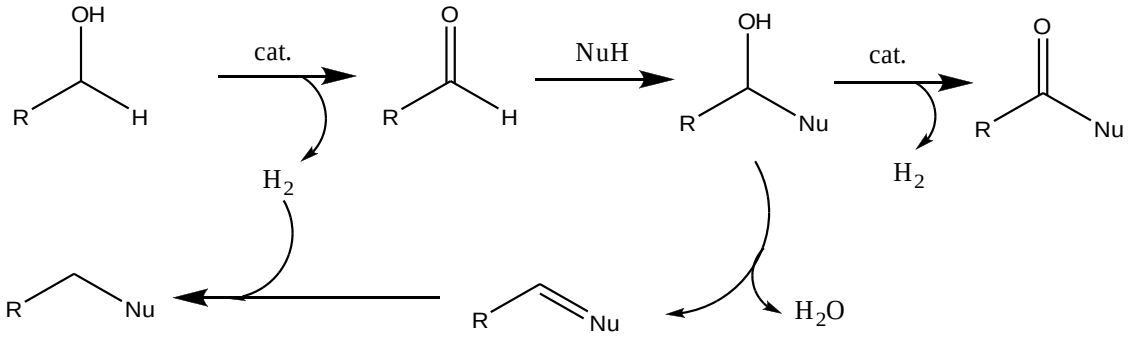

Nu = nucleophile

Scheme 4. Acceptorless dehydrogenation of primary alcohols: nucleophilic attack.

1.2.2. Acceptorless alcohol dehydrogenation

The catalytic systems (metal complexes) that support this type of reaction have been thoroughly investigated and the results reported in the literature can be divided into two different categories, depending on the role played by the ligand. If the ligand takes part in the catalytic cycle (for example coupled in the redox reaction, with a change in its oxidation state), it is called “non-innocent ligand”; if instead the ligand is not part of the catalytic cycle, it is called “innocent ligand”. The latter type has however different roles in ensuring complex stability, appropriate electronic configuration, and steric bulkiness to the organometallic complex.

1.2.2.1. Metal complexes with innocent ligands

In 1987, aiming at producing hydrogen from biomass, Morton and Cole-Hamilton reported one of the first catalysts used for acceptorless dehydrogenation of alcohols[30], $[Rh(bipy)_2]Cl$ (bipy = 2,2'-bipyridine). In particular, they investigated the oxidation of ethanol (one of the major products derived from biomass), establishing that it is a thermodynamically uphill process that has to work in an open system at high temperatures.

Following this route, the same team showed that ruthenium dihydride complexes can be useful catalysts to dehydrogenate primary alcohols and diols[31-32]. For ethanol dehydrogenation, in the presence of a base (e.g. NaOH), the catalyst $[RuH_2(N_2)(PPh_3)_3]$ (**2a**) showed a TOF of 148.1 h^{-1} (210.2 h^{-1} upon illumination), whereas catalyst $[RuH_2(PPh_3)_4]$ (**2b**) showed a TOF of 23.8 h^{-1} (138.7 h^{-1} under illumination). The proposed mechanism is shown in Scheme 5.

After the release of a ligand to get a free coordination site, the 16 e^- complex **A** is attacked by an ethoxide ion to give the alkoxyruthenium complex **B**. This complex releases acetaldehyde by β-H elimination, and is converted in the trihydride complex **C**. This complex is then protonated by an alcohol molecule to give the tetrahydride complex **D**, that is supposed to release molecular hydrogen by reductive elimination.

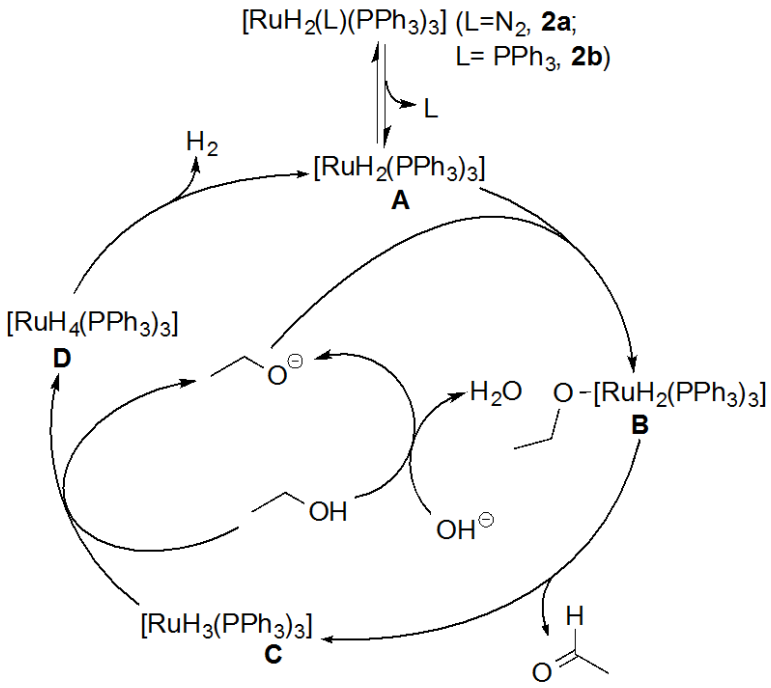

Scheme 5. Mechanism for primary alcohol dehydrogenation proposed by Morton and Cole-Hamilton.

Recent studies have proved that the addition of free PPh_3 inhibits the reaction, indicating that the ligand dissociation is involved in the reaction mechanism[33]. For both rhodium and ruthenium complexes the addition of a base is a crucial step to reach high catalytic activities. The base has two main functions: the first one (as seen previously) is to promote proton dissociation to generate the alkoxide ion, which in turn reacts with complex **A**.

Following this route, dehydrogenation of methanol was studied using several ruthenium(II)-phosphine complexes[33]: $[RuCl_2(P(p\text{-}C_6H_4X)_3)_3]$ (X= H; Me; F; OMe) and $[RuCl_2(PMePh_2)_3]$. The results showed that the produced formaldehyde reacted immediately to form acetals and esters (Scheme 6). Again, addition of free phosphine retarded the reaction, suggesting that ligand dissociation takes place during the catalytic cycle.

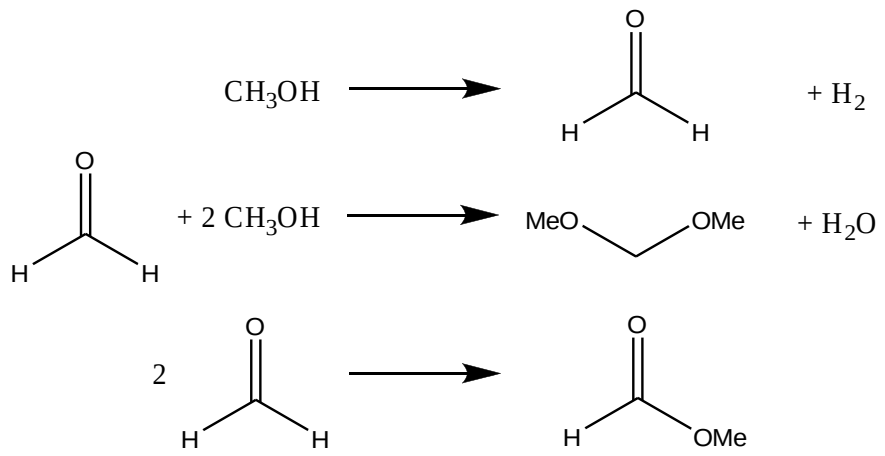

Scheme 6. Acceptorless dehydrogenation of methanol.

Recently, Beller and Junge investigated the use of *in situ* formed ruthenium catalysts for the dehydrogenation of *iso*-propanol at 90 °C[33-34]. Among the different ruthenium precursors screened, $[RuCl_3 \bullet xH_2O]$ and $[RuCl_2(p\text{-cymene})]_2$ showed to be the most active in the presence of two equivalents of tricyclohexylphosphine, PCy_3. In particular, the best catalytic performance was obtained by using $[RuCl_3 \bullet xH_2O]/PCy_3$ (1:2) in the presence of metallic sodium as a base instead of NaOH (TOF = 101 h^{-1} after 2h and 57 h^{-1} after 6 h).

The same group also analyzed ruthenium complexes with amine instead of phosphine ligands. Various mono-, bi-, and tridentate nitrogen ligands were investigated for the dehydrogenation of *iso*-propanol in the presence of $[RuCl_2(p\text{-cymene})]_2$ and NaO*i*Pr. In the presence of most of the tested nitrogen ligands, TOFs higher than 200 h^{-1} after 2 h and higher than 100 h^{-1} after 6 h were obtained.

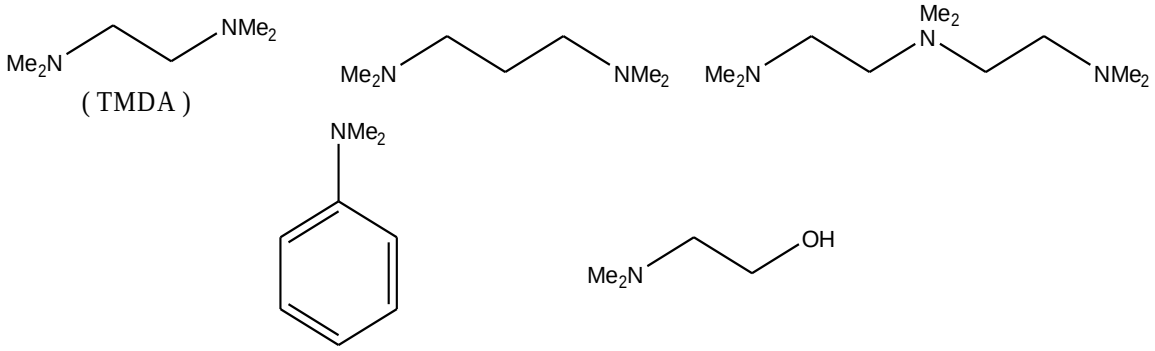

*Figure 7. Nitrogen ligands used for the dehydrogenation of isopropanol in the presence of [RuCl2(*p*-cymene)]2 and NaO*i*Pr.*

An interesting discovery coming out from these works was that decreasing the catalyst loading from 16 ppm to 4 ppm and increasing the ligand:catalyst ratio to 10:1, the highest TOFs were obtained (519 h^{-1}, 317 h^{-1} and 189 h^{-1} after 2, 6 and 24 hours).

1.2.2.2. Metal complexes with non-innocent ligand

A. Historical background

In 1977, Dobson and Robinson developed one of the earliest catalyst for acceptorless dehydrogenation of primary and secondary alcohols[35-36]. Using an excess of fluorinated carboxylic acid (acid promoter) they found a very active Ru(II)-complex: $[Ru(OCOCF_3)_2(CO)(PPh_3)_2]$. This could dehydrogenate 1-heptanol and cyclooctanol with a TOF of, respectively, 2952 h^{-1} and 1620 h^{-1} with a catalyst loading of 0.03%. TOFs for smaller primary and secondary alcohols were found to be lower than 100 h^{-1}, probably due to the lower reaction temperature.

This catalytic system represents an early example of non-innocent ligand application. The proposed catalytic cycle starts by the addition of the alcohol onto the $[Ru(OCOCF_3)_2(CO)(PPh_3)_2]$, which changes the coordination of the trifluoroacetate from η_3 to η_1. The coordinated alcohol is believed to be hydrogen-bonded to one of the η_1 trifluoroacetate ligands, in analogy to isolated $[Ru(OCOCF_3)_2(CO)(PPh_3)_2(RR'CHOH)]$ **A** complex[37]. Dissociation of trifluoroacetic acid leads to the formation of an alkoxide complex $[Ru(RR'CHO)(OCOCF_3)(CO)(PPh_3)_2]$ **B**. In this process, the ligand plays an active role and it is directly involved in the steps leading to the alkoxide complex. In the following step, the alkoxide is transformed into the corresponding carbonyl by β-H elimination leading to the hydride complex $[RuH(RR'CO)(OCOCF_3)(CO)(PPh_3)_2]$ **C**. Attack of trifluoroacetic acid onto the hydride complex liberates the carbonyl product together with molecular hydrogen, hence closing the catalytic cycle by forming the starting ditrifluoroacetate complex $[Ru(OCOCF_3)_2(CO)(PPh_3)_2]$.

After a few years, in 1982, Jung and Garrou tried to reproduce the results of Dobson and Robinson, replacing triphenylphosphine by diphosphine ligand in $[Ru(OCOCF_3)(CO)(PPh_3)_2]$[38], but they were unable to do it. They proposed that the reasons for non-reproducibility was catalyst deactivation caused by decarbonylation of the aldehyde that produces inactive metal carbonyl compounds, and the evaporation of the required trifluoroacetic acid (no longer available to assist the metal in the catalytic cycle) under reaction conditions.

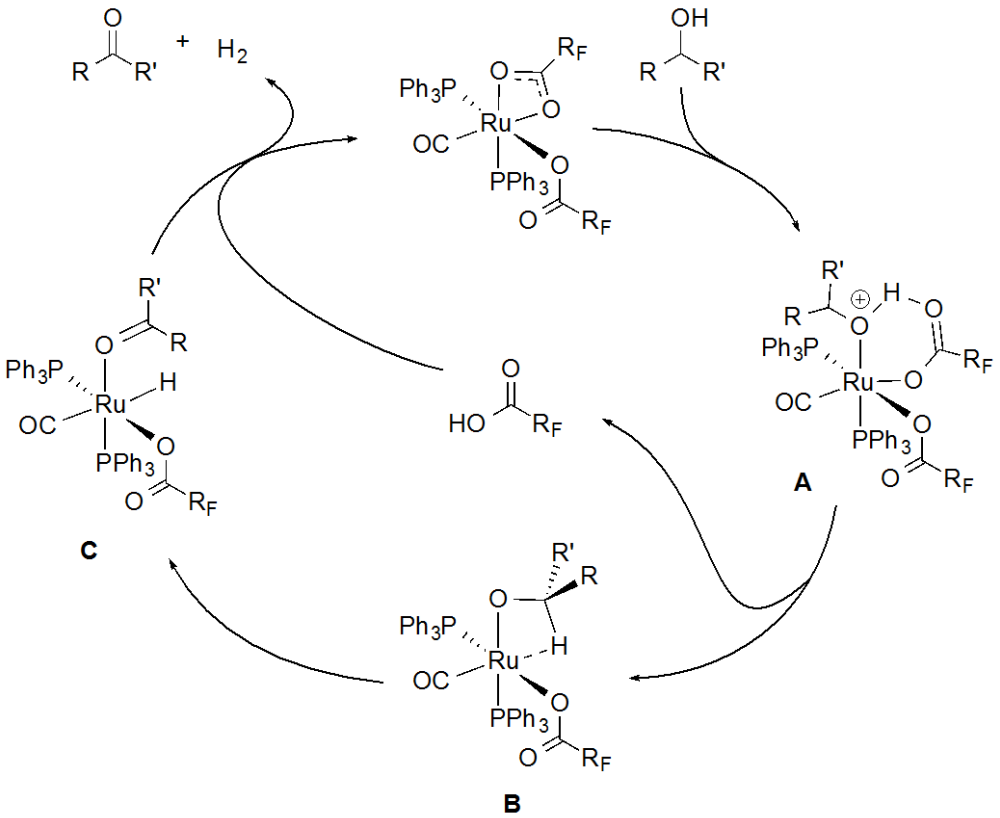

Scheme 7. Catalytic cycle for acceptorless alcohol dehydrogenation proposed by Dobson and Robinson.

In the same years, Shvo and his team synthesized a dinuclear ruthenium complex that found lots of applications in oxidation and reduction reactions.

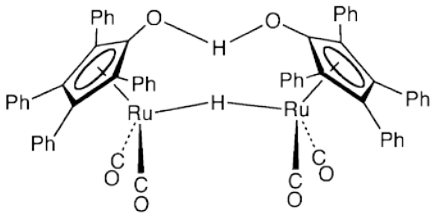

Figure 8. Shvo's diruthenium complex.

In solution, the dimer dissociates into two complexes: one saturated (that takes the hydrogen previously bonded to both Ru centers, and the OH-group bonded to the aromatic ring) and the other unsaturated (with a vacant coordination site instead of hydrogen, and a double bond with the oxygen on the aromatic ring). Both complexes can interconvert into each other by hydrogenation of a hydrogen acceptor (A) or dehydrogenation of a hydrogen donor (AH_2). Shortly before the isolation and structural determination of the ruthenium

dimer, Shvo reported the acceptorless dehydrogenation of 2-octanol and cyclohexanol at 145 °C using a ruthenium dimer described as $[(\eta_4\text{-}Ph_4C_4CO)Ru(CO)_2]_2$[36]. More recently, Shvo's catalyst was used for dehydrogenation of 1-phenylethanol leading to up to 98% of acetophenone[38]. The catalyst was hetereogenized by entrapment of the dimer using a sol-gel process. The heterogeneous catalyst was found to be slightly more active than the homogeneous complex and it could be recycled up to 5 times maintaining 87% of its initial activity.

B. New catalytic systems: metal with non-innocent PNP and PNN pincer ligands

Since 2010, Milstein and co-workers have carried out a pioneering work on the use of aromatic PNP and PNN pincer ligands in cooperative metal-ligand catalysis[28][39-40-41]. The reactivity of this type of complexes relies on cooperation between the metal and the aromatized-dearomatized ligand for the reversible activation of chemical bonds (Scheme 8). This process does not influence the formal oxidation state of the metal center because the nitrogen atom of the pyridine ring switches from a two-electron donor amino ligand to a one-electron donor (en)amido ligand. These type of catalysts were firstly investigated for the acceptorless hydrogenation of secondary alcohols to the corresponding ketones, with dioxane as solvent in the presence of a base[42].

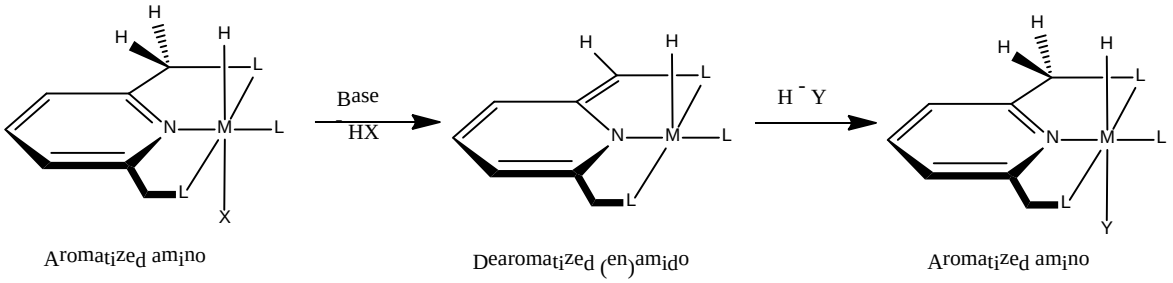

Scheme 8. Activation of Milstein's catalysts

In the last years, Beller and his group followed this route to study hydrogenation of alcohols catalyzed by ruthenium aromatic and aliphatic PNP pincer complexes, targeting hydrogen production[43]. As with the corresponding aromatic complexes, aliphatic Ru-PNP pincer complexes are able to activate chemical bonds by metal-ligand cooperation. The mechanism is similar to the previous one: the nitrogen atom switches from a two-electron donor amino ligand to a one-electron analogue (Scheme 9).

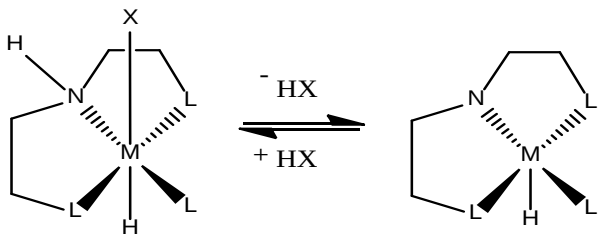

Amino Amido

X = H, Cl, Br, OH, OR, NH_2, NR_2, alkyl, aryl
L = 2e- donor atom

Scheme 9. Activation of LNL-Ru catalysts.

Beller's team tested isolated ruthenium de-aromatized PNN complex **B1** and aliphatic complex **B2**, together with *in situ* formed catalysts produced by reaction between Ru-sources (**B3** and **B4**) and aliphatic PNP ligands (**B5**, **B6**, and **B7**).

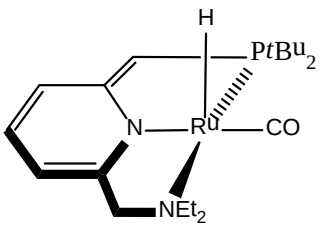

B1

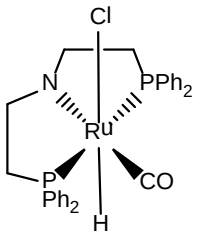

B2

$[RuHCl(CO)(PPh_3)_3]$

B3

$[RuH_2(CO)(PPh_3)_3]$

B4

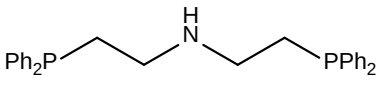

B5

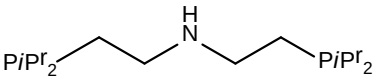

B6

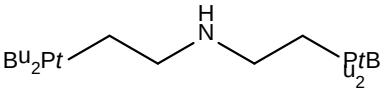

B7

Figure 9. Selected examples of Beller's catalysts.

Catalysts' activity was evaluated by monitoring evolution of H_2 over time. Catalysts **B1** and **B2** showed similar activities, but, for **B2**, a reduction in the amount of the added base (NaO*i*Pr, equimolar ratio) improved its catalytic performance; on the contrary, without base, complex **B2** proved to be inactive, presumably because the active catalytic species is formed only after elimination of HCl by the base. *In situ* formed catalysts derived from an equimolar mixture of **B3** and aliphatic PNP pincer ligands **B5** or **B6** were found to be active with 1.3 equivalents of NaO*i*Pr. The nature of the substituents on the phosphorous atom strongly influences catalytic activity, that increases when the phenyl

group is substituted by more electrons donating *i*-propyl substituents, with a TOF, after 2 hours, of 460 h^{-1} and 1187 h^{-1} for **B3/B5** and **B3/B6**, respectively. The most active catalytic species obtained is the *in situ* complex derived from the dihydride species **B4** and the aliphatic PNP **B6**, with a TOF of 8382 h^{-1} after 2h, without any additional base.

The general conclusions that can be drawn from this work are very interesting:

- Phosphorous substituants strongly influence catalysts' activity, with more electron donating groups (like isopropyl) leading to higher reaction's rate,
- Additional base is not always needed, only if the elimination of a substituent (for example an halide) is necessary to obtain an active catalytic species,
- PNP and PNN pincer ligand show the highest activities in terms of reaction rate, expressed by TOFs, for the dehydrogenation of secondary alcohols,
- Even if the system is active at low reaction temperatures (90°C), the conversion observed is very low (<20%) and the reaction stops after 6 hours.

Beller proposed a mechanism for the *in situ* formed complex **B4**/**B6**, which provides for the formation of an unsaturated 16 e^- complex after molecular hydrogen extrusion, that is propose to dehydrogenate the alcohol via an outer-sphere mechanism involving both the ruthenium center and the PNP ligand nitrogen atom.

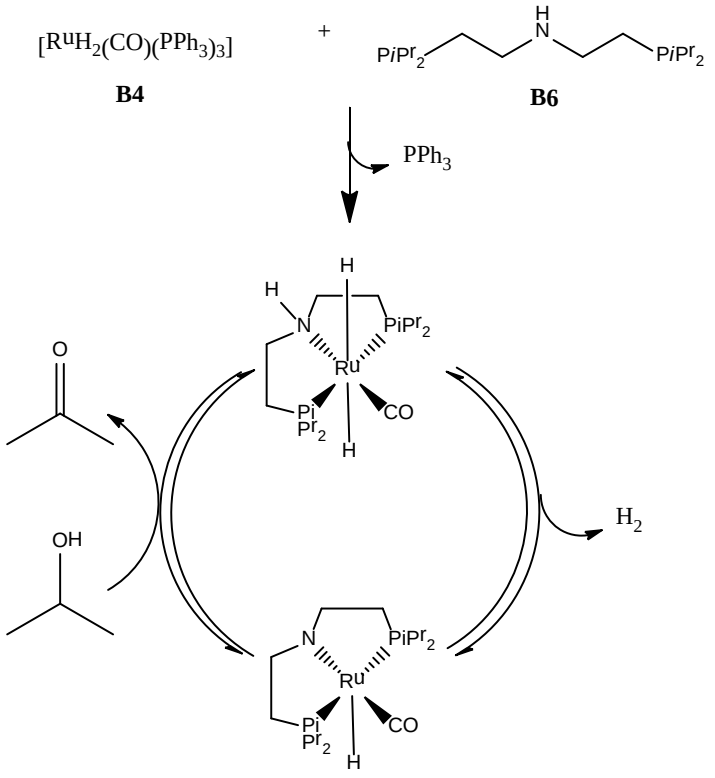

Scheme 10. Beller's proposed mechanism for Ru-complex activation.

1.2.3. Acceptorless dehydrogenative coupling of primary alcohols

1.2.3.1 Introduction

While the dehydrogenation of secondary alcohols leads to ketones, the same reaction for primary alcohols do not lead to aldehydes, but it usually proceeds through the formation of esters.

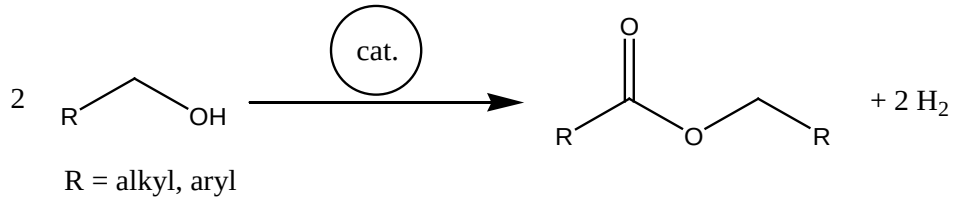

Scheme 11. Acceptorless dehydrogenative coupling of primary alcohols.

The reason for this behavior is that the produced aldehyde is very reactive and quite unstable, and it immediately reacts with another alcohol molecule to give an hemiacetal that is further dehydrogenated to give an ester.

To have a useful comparison between different catalytic systems, we can identify some starting points based on considerations arising from the different characteristics of the complexes seen so far for the acceptorless alcohol dehydrogenation:

- due to thermodynamics and kinetics reasons, the substrate reactivity toward dehydrogenation usually decreases in the order: aromatic secondary alcohol > aliphatic secondary alcohol > benzyl alcohol > aliphatic primary alcohol;
- in most reported cases, a base (or sometimes an acid) and an organic solvent are required for the evolution of the reaction;
- regarding catalytic performance evaluation, both turnover frequency and product yield are crucial factors. A strongly efficient catalytic system should give at the same time a high TOF (i.e. a high reaction rate) and a high product yield (with high selectivity, conversion, and catalyst stability).

Based on these guidelines, we can say that the most challenging transformation appears to be the alcohol dehydrogenative coupling under neutral and neat conditions, with the most unreactive substrates being primary alcohols. Short chain primary alcohols derived from biomass, ethanol and butanol in particular, are the most widely available in nature and they will be the subjects of the present thesis.

1.2.3.2. Historical background

In the early eighties, Shvo and his team developed one of the first examples of dehydrogenative coupling of alcohols to esters[44-45], showing that $Ru_3(CO)_{12}$, in the presence of both 1,2-diphenylacetylene and Shvo's dimer (describer above), could accomplish dehydrogenative coupling of alcohols in the absence of any acceptor[46]. Murahashi found that the complex $[RuH_2(PPh_3)_4]$ was able to catalyze the acceptorless transformation of aliphatic alcohols to esters without the presence of any base at high temperature (180 °C)[47]. As previously seen, a new generation of Ru-based PNP and PNN pincer complexes, based on the metal-ligand cooperation, was discovered first by Milstein's group, and successively investigated by Gusev's and Beller's groups; finally, this will be the object of the present thesis.

1.2.3.3. Milstein's catalysts

In the last decade, Milstein and co-workers have found a large variety of Ru-based catalysts bearing aromatic pincer PNP, PNN and PNNP ligands, useful for the dehydrogenation and dehydrogenative coupling of alcohols (Figure 10).

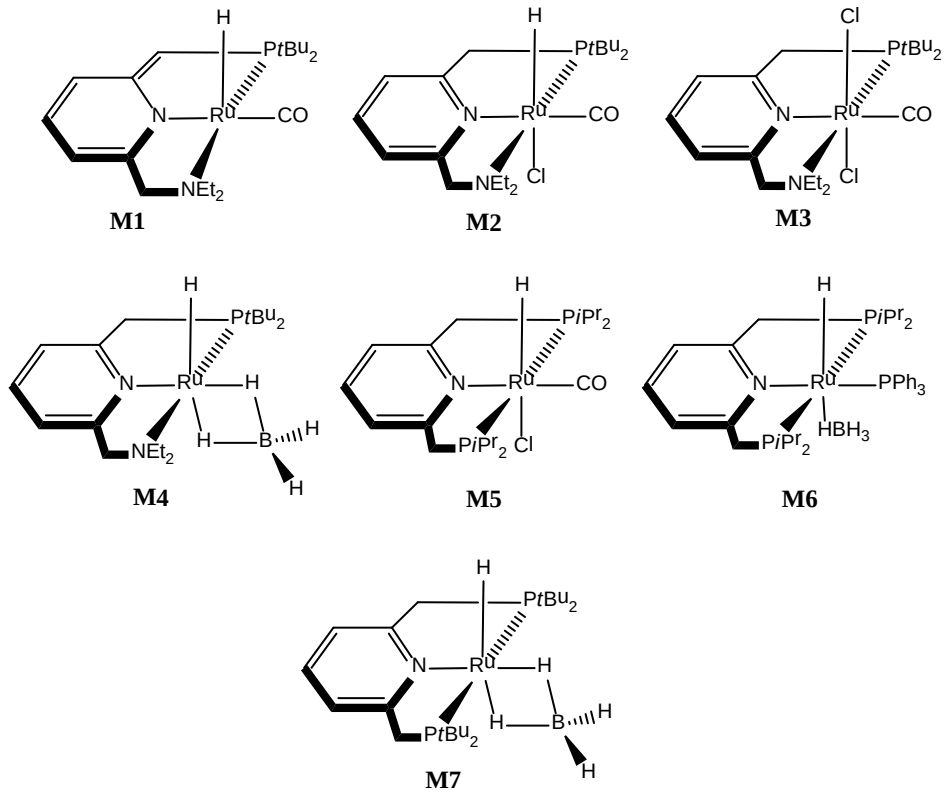

Figure 10. Selected examples of Milstein's catalysts

Milstein *et al*. investigated catalytic activities for the reaction with 1-hexanol and 1-butanol. Their results are reported in Table 1.

entry	cat. (mol %)	substrate	base (mol%)	solvent	temp (°C)	time (h)	yield (%)	ref
1	**M1** (0.1)	1-hexanol	/	/	157	2.5	91.4 to ester 0.5 to aldehyde	[48]
2	**M2** (0.1)	1-hexanol	/	/	157	24	/	[48]
3	**M2** (0.1)	1-hexanol	KOH (0.1)	/	157	24	90.4 to ester 0.3 to aldehyde	[48]
4	**M3** (0.1)	1-hexanol	NaO*i*Pr (0.2)	dioxane	100	24	91 to ester 0.5 to aldehyde	[49]
5	**M4** (0.1)	1-hexanol	/	toluene	115	24	94 to ester No aldehyde	[50]
6	**M5** (0.1)	1-hexanol	KOH (0.1)	/	157	24	67.2 to ester 2.8 to aldehyde	[48]
7	**M6** (0.1)	1-hexanol	/	/	157	24	47 to ester 10 to aldehyde	[50]
8	**M7** (0.1)	1-hexanol	/	toluene	115	24	69 to ester 3 to aldehyde	[50]
9	**M1** (0.1)	1-butanol	/	/	117	5	90 to ester 0.5 to aldehyde	[48]
10	**M4** (0.1)	1-butanol	/	toluene	110	24	96 to ester No aldehyde	[50]

Table 1. Catalytic activities of Milstein's catalysts for dehydrogenative coupling of 1-hexanol and 1-butanol.

From the Table 1 we can observe that, upon addition of one equivalent of base to **M2** (entry 3), 90.4% of hexyl hexanoate is obtained after 24 hours reflux: but in the absence of the base (entry 2), no reaction is observed. This confirms that elimination of HCl from the inactive aromatic PNN Ru-complex **M2** to give the dearomatized active complex **M1** is a crucial point. Supporting this, it can be seen that similar yields are obtained using complex **M1**(entry 1), **M2**+KOH (entry 3) and **M3**+NaO*i*Pr (entry 4).

Another important discovery regards aromatic PNP and PNN pincer ruthenium complexes bearing borohydrides ligands instead of chlorides (**M4**, **M6**, and **M7**). These complexes, where borohydrides are "masked" hydrides, are very active for the dehydrogenative coupling of both primary alcohols without additional base. Perhaps, their mechanisms involve elimination of molecular hydrogen upon thermal activation to give the active dearomatized species.

According to the authors, PNN complexes are more active species than the corresponding PNP derivatives, this is probably due to the easier decoordination of the amine arm in the PNN ligand. The ligand dissociation step is crucial, necessary to create a vacant site on the metal, hence to allow the following β-elimination step to take place (Scheme 12). Of course, this step is facilitated when the lost ligand is not strongly coordinated to the metal center.

As far as the reaction with butanol is concerned, the best performances are reached with 0.1 mol% of complex **M1** under neat and neutral conditions, with a yield of 90% in butyl butyrate after 5 hours, which corresponds to a TON of 900 and a TOF of 180 h^{-1}.

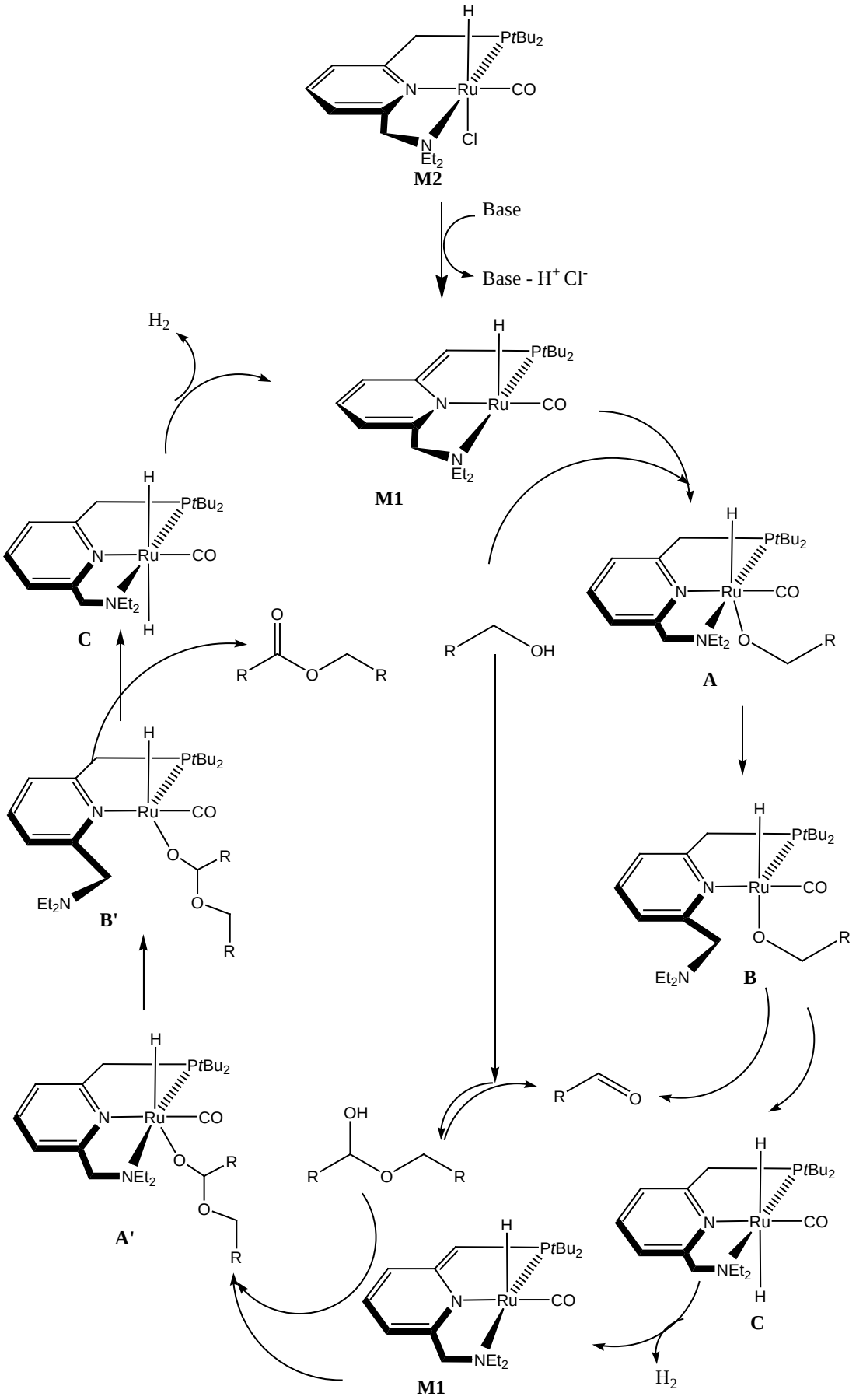

Scheme 12. Milstein's proposed mechanism for acceptorless dehydrogenative coupling of alcohols.

1.2.3.4. Gusev's catalysts

Gusev and co-workers developed several different ruthenium and osmium complexes for the dehydrogenative coupling of primary alcohols. Most of them presented a tridentate pincer ligand having a functional NH group spaced by two carbon atoms from the phosphorous, nitrogen, or sulfur donor atoms (Figure 11).

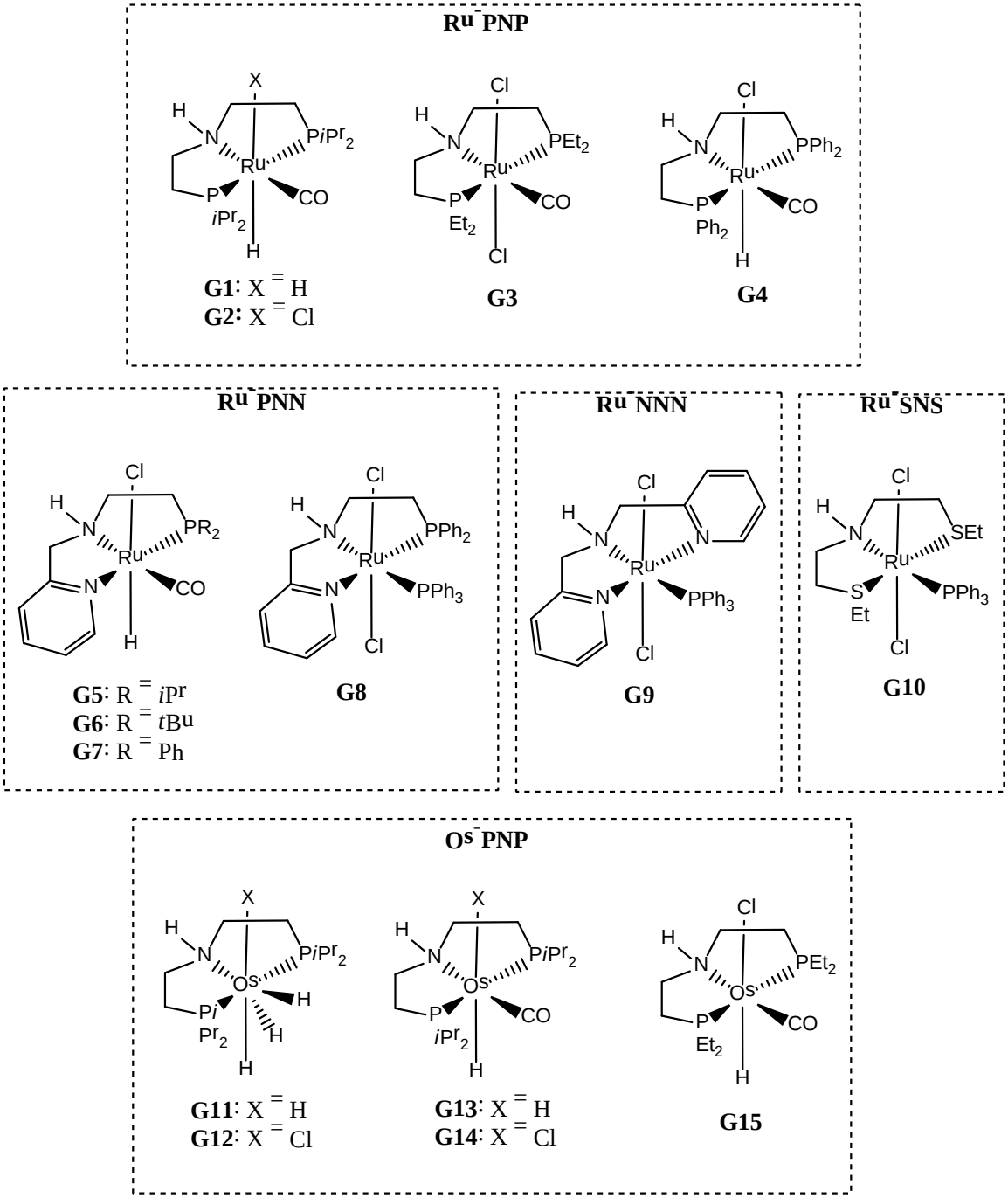

Figure 11. Gusev's ruthenium and osmium complexes tested for alcohol dehydrogenative coupling.

entry	cat. (mol %)	base (mol %)	substrate	Temp. (°C)	Time (h)	Yield (%)	Ref.
1	**G1** (0.1)	/	1-butanol	118	6	21	[52]
2	**G2** (0.05)	NaOEt (0.1)	ethanol	78	16	57	[51]
3	**G2** (0.1)	NaOEt (0.1)	ethanol	78	24	47	[51]
4	**G4** (0.1)	NaOEt (0.1)	ethanol	78	24	47	[51]
5	**G4** (0.005)	NaOEt (0.1)	ethanol	78	40	42	[51]
6	**G3** (0.05)	NaOEt (0.1)	ethanol	78	16	17	[51]
7	**G5** (0.1)	*t*BuOK (0.5)	ethanol	78	7.5	30	[53]
8	**G5** (0.1)	*t*BuOK (0.5)	1-butanol	118	3	78	[53]
9	**G6** (0.05)	NaOEt (0.1)	ethanol	78	16	12	[51]
10	**G7** (0.05)	NaOEt (0.1)	ethanol	78	16	41	[51]
11	**G7** (0.1)	NaOEt (0.1)	ethanol	78	24	42	[51]
12	**G8** (0.05)	NaOEt (0.1)	ethanol	78	16	95	[51]
13	**G8** (0.1)	NaOEt (0.1)	ethanol	78	24	91	[51]
14	**G8** (0.005)	NaOEt (0.1)	ethanol	78	40	85	[51]
15	**G9** (0.05)	NaOEt (0.1)	ethanol	78	16	0	[51]
16	**G10** (0.05)	NaOEt (0.1)	ethanol	78	16	97	[61]
17	**G10** (0.01)	NaOEt (0.1)	ethanol	78	24	89	[61]
18	**G11** (0.1)	/	ethanol	78	5	3	[54]
19	**G11** (0.1)	/	1-butanol	118	8	3	[54]
20	**G12** (0.05)	NaOEt (0.1)	ethanol	78	16	2	[51]
21	**G13** (0.1)	/	1-butanol	118	7	6	[52]
22	**G14** (0.05)	NaOEt (0.1)	ethanol	78	16	23	[51]
23	**G15** (0.05)	NaOEt (0.1)	ethanol	78	16	30	[51]

Table 2. catalytic activities of Gusev's complexes.

From the catalytic activities described for several ruthenium and osmium complexes (Table 2) , some structural-activity relationship can be drawn:

- the use of an additional base seems crucial to obtain active catalysts (Table 2, entry 1, 18, 19, 21: without any base, reaction yields are very low);
- osmium-based catalysts are usually less active then the corresponding ruthenium species (entry 18 ÷ 23);
- for hydridochlororuthenium PNP complexes, the nature of the substituents at the phosphorous atom does not seem to affect significantly catalytic activities (entry 3 and 4);
- dichlororuthenium complex **G3** proved to be less efficient than hydridochlororuthenium complexes **G2** and **G4**, although substituents on the P-atom are different;

- when replacing PNP ligand with PNN or SNS, no significant differences in activity were found, however with an NNN ligand having two pyridine moieties, no catalytic activity was observed;
- for PNN complexes, substitution of the carbonyl ligand *trans* to the NH group by a triphenylphosphine ligand strongly improves catalytic activities (entries 10 vs 12 and 11 vs 13);
- catalyst loading is important for the outcome of the reaction: a decrease in catalyst concentration brought about an improvement in reaction rate and yield[51].

Based on experimental and computational results, Gusev *et al.* proposed an outer-sphere reaction mechanism for Ru-PNP complexes, involving a 16 e^- amido metal complex[52-53,54]. After the reaction with a base, the hydridochloro metal complexes **G2** and **G4** release HCl to give the unsaturated amido metal complex **A**, which is then protonated by an alcohol molecule at the nitrogen atom of the ligand, to give a cationic complex $[RuH(CO)(PNHP)]^+$ **B**, connected to an alkoxide ion RO^- via an $O^{\cdots}H$-N hydrogen bond and an agostic C-$H^{\cdots}$M interaction. This species is in equilibrium with an alkoxyruthenium complex **B'** (isolated and fully characterized by Gusev's team[52]). From complex **B** the hydride is transferred to the metal center to give the aldehyde product and the metal dihydride RuH_2. The extrusion of molecular hydrogen occurs in two steps, involving a dihydrogen intermediate **C** (highest activation energy: $\Delta G^{\neq}$ = 29.2 kcal/mol, rate determining step). However, the assistance of an alcohol molecule decreases the energy barrier for the formation of this complex.

Similar observations were reported by Schneider, who investigated the dehydrogenation of complex $[RuH_2(PMe_3)(i Pr_2PCH_2CH_2)_2NH]$ to the unsaturated amido complex $[RuH(PMe_3)(i Pr_2PCH_2CH_2)_2N)]$ assisted by a water molecule[55].

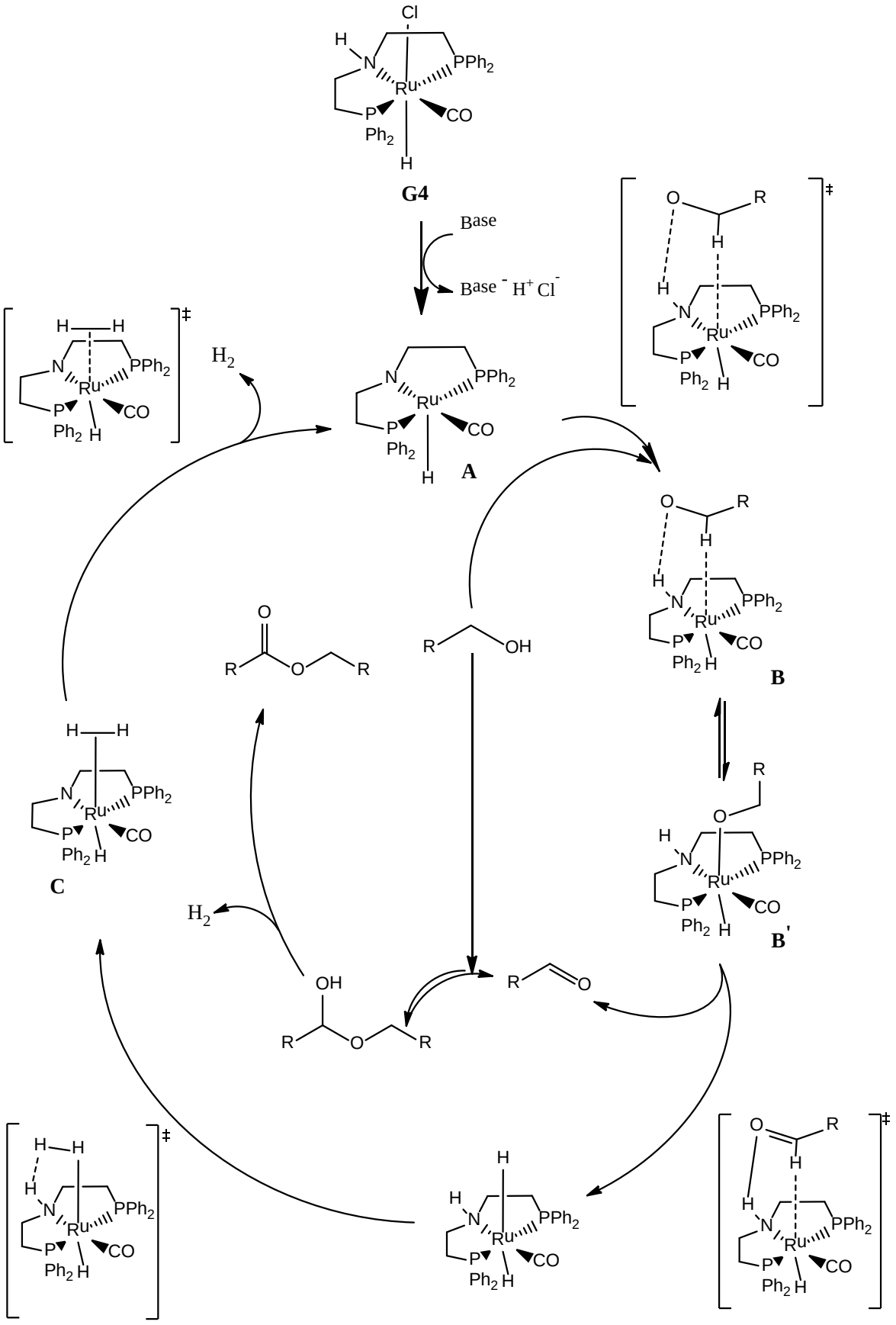

*Scheme 13. Proposed mechanism for the acceptorless dehydrogenative coupling of alcohol by Gusev's catalyst **G4**.*

1.2.3.5. Beller's catalysts

As previously reported, Beller and co-workers used a series of *in situ* catalysts and commercially available ruthenium complexes for the dehydrogenative coupling of ethanol[56].

entry	cat. (ppm)	base (mol %)	time (h)	yield (%)	TOF (h^{-1})	TONmax (time)	ref
1	**B4/B6** (3.1)	/	2	0.9	1483	4140 (6h)	[43]
2	**B4/B6** (3.1)	/	6	1.3	690		[43]
3	**B2** (500)	EtONa (1.3)	2	49.8	498	1620 (6h)	[56]
4	**B2** (500)	EtONa (1.3)	6	81	270		[56]
5	**B2** (50)	EtONa (0.6)	2	9.3	934	15400 (46h)	[56]
6	**B2** (50)	EtONa (0.6)	10	36.5	730		[56]
7	**B2** (50)	EtONa (0.6)	46	77	335		[56]

Table 3. Catalytic activities of Beller's complexes.

Catalytic tests with *in situ* formed catalyst **B4**/**B6** (Figure 9) were performed without any base or solvents, using ethanol as substrate and very low catalyst loading (3.1 ppm). A high turnover frequency (1483 h^{-1}) was found after 2 hours, but it significantly decreased after 6 hours, indicating that deactivation of the catalyst was occurring. An interesting fact regards the yields, which decreased for very high TOFs.

The reaction was also performed with the isolated complex **B2**, in presence of a base, at different concentrations, with different catalyst loadings. The best performances were obtained with 500 ppm of complex **B2** and 1.3 mol% of NaOEt (81% yield after 6 hours).

An important consideration concerns catalyst concentration: when decreasing catalyst loading from 500 to 50 ppm, reaction rate was strongly increased from a TOF of 498 to 934 h^{-1}. Thanks to those considerations, Beller and his group reported a hypothetical catalytic cycle, similar to the one described for the dehydrogenation of alcohols.

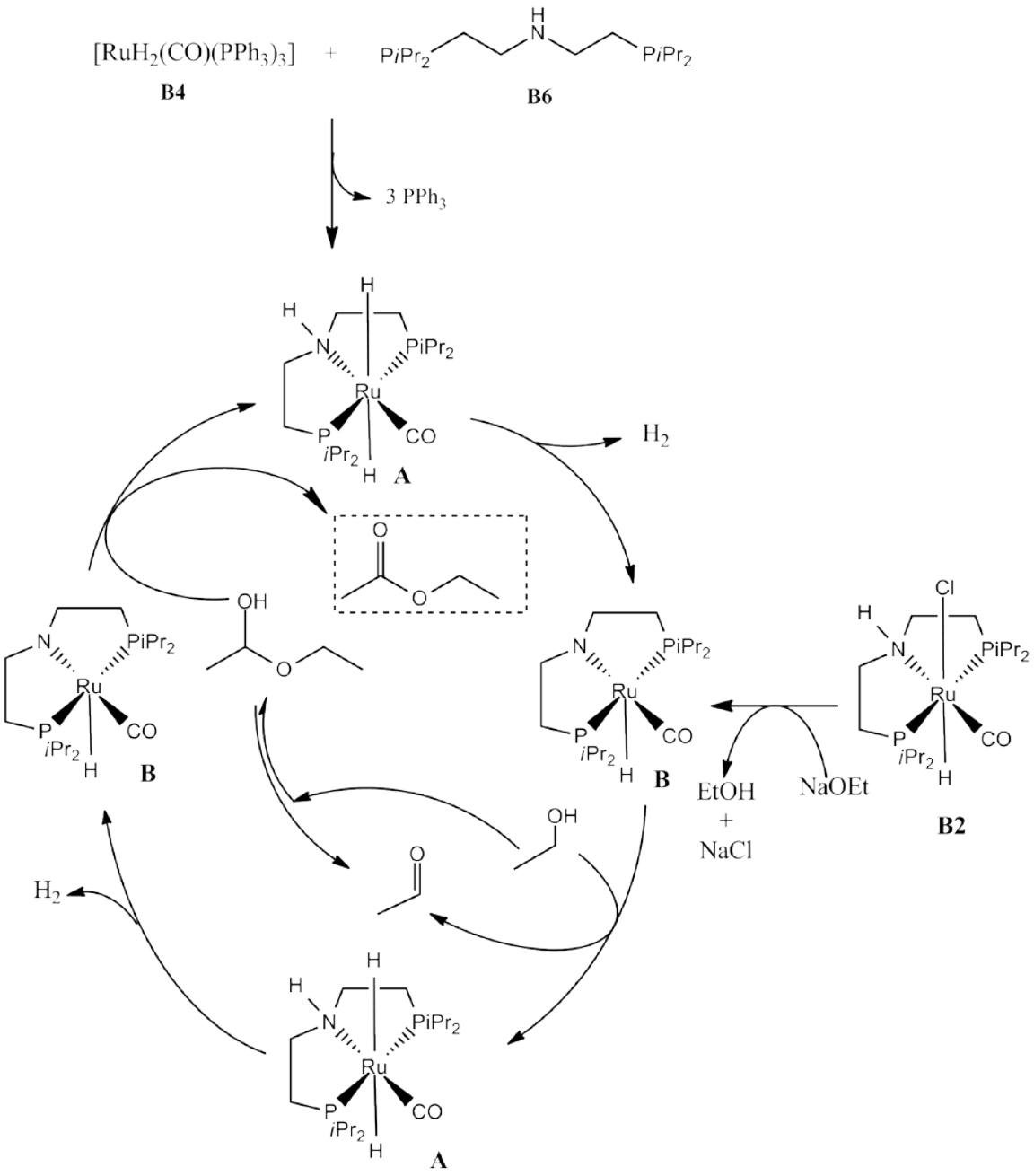

Scheme 14. Beller's proposed catalytic cycle for ethanol dehydrogenative coupling.

1.2.3.6. Conclusions

In the last decades, several catalytic systems have been studied for primary alcohols dehydrogenative coupling. Looking at the results obtained by the different research groups listed above, it is possible to identify some key issues and expectable improvements. PNP pincer ligands seem to be the more suitable to give active ruthenium complexes. This arise firstly from their bulkiness, that gives the complex the right steric hindrance that permits dissociation of the ligand on the top of the Ru center (as identified in all reaction mechanisms) and the creation of the vacant site of coordination that triggers the catalytic cycle. However, this is not a specific characteristic of PNP ligand, since PNN are active too. But PNP ruthenium system offers unusual 2-fold metal-ligand cooperativity, both at the hydrogen atom and the ligand backbone. This bifunctional catalyst bears a cooperative amino ligand which is specifically involved in the catalytic cycle via reversible chemical transformations (Scheme 9) without changes in the formal oxidation state of the ruthenium centre.

On the other hand, most of the catalytic complexes seen so far worked only in presence of a base and sometimes of an organic solvent: this would lead to waste and separation problems. To evaluate the ideal catalyst for dehydrogenative coupling of primary alcohols, we have to consider both the conditions of the reaction (base- and solvent-free), both thermodynamic and kinetic factors (i.e. TON, TOF, yield, and conversion).

2. Purpose of the project

Acceptorless dehydrogenative coupling of primary alcohols is an environmentally friendly, atom-efficient route to produce symmetrical esters. In this reaction, the only byproduct is molecular hydrogen, which is directly usable as a clean energy source and a neat reduction agent. Despite the recent growing interest in this kind of transformations, the overall process still requires improvements.

In order to gain an insight on this transformation, 1-butanol was used as a model substrate of short-chain primary alcohol, because of its easier handling (higher boiling point than ethanol, 118 °C vs 78 °C) and its wide availability on the market (first and second generation biomass). For sake of completeness, it is hereby given that this project is part of a wider project, followed by the research group of Doc. Simon Desset (UCCS, Unité de Catalyse et Chemie du Solide, Université de Lille 1 - Sciences et Technologies). All the reported results have been confirmed by independent experiments carried out by group members. Parallel work on ethanol has been object of a patent[62].

2.1. New catalysts

Starting from Milstein's, Gusev's, and Beller's works, a new series of Ru-PNP pincer complexes were developed. Both *in situ* and isolated complexes were studied, focusing on the role of different ligands, in order to establish their influence on the catalytic activities of the complexes. In particular, the present work aimed at investigating the influence of the different substituants on the phosphorous atoms of PNP binder, the ligand in the *trans*-position relative to the NH group of PNP, and, most important, the ligand *trans* to the hydrogen. The latter appears to be the most critical, since, according to the mechanism proposed by different research groups (previously reported), the initial ligand release is required to leave a vacant site that allows for the catalytic cycle to start.

A known efficient commercial catalyst for this type of reaction is Ru-MACHO-BH, a very expensive complex (ca. 600 €/ 5 g) produced by Takasago Fine Chemicals Division. This high price clearly points to a search for new and cheaper catalysts, possibly starting from "green" and simple reactants, capable of comparable performances.

The features required for active catalysts useful for the development of the project are:

- activity and selectivity for the reaction;
- reaction rate and other kinetic and thermodynamic factors (TON, TOF, yield and

conversion);

- possibility of working without the need for any additional base or solvent;
- stability of the catalyst and reproducibility of the results;
- economic factors, i.e. cost of the catalyst (for commercial ones) or costs of the precursors (for *in situ* formed catalysts).

2.2. Hydrogen transfer limitations

Previous works have evidenced the influence of catalyst concentration on the rate and the general course of the reaction. For low catalyst loading, the highest catalytic activities have been recorded, but, under those conditions, low conversions and yields were obtained. This fact is amenable to two factors: the extrusion of molecular hydrogen out of the liquid phase[53], and to the ease of deactivation of the catalyst by reaction with molecular oxygen from the external atmosphere (at low catalyst loading the reaction requires more time to reach completion which facilitates slow external contaminations).

The equilibrium of the reaction seems to be controlled by the extrusion of H_2, which must be correctly removed from the reaction media to ensure proper reaction kinetics. At high catalyst loadings, large flows of H_2 are produced, and, if not efficiently removed from the liquid phase, it shifts the reaction equilibrium. Therefore, the catalyst loading has to be adjusted in accordance with the capacity of the reactor to develop enough gas-liquid exchange to release the produced H_2. In general, the best conditions to remove hydrogen from the system involve a very high stirring rate, baffles, and reflux conditions in an open system.

As far as the reactor is concerned, three different types were tested, in order to minimize contact with external contaminants, to ensure that reaction is under chemical regime and to maximize reproducibility of the results.

3. *Experimental part*

3.1. Materials

Molecular sieves 3Å (SIGMA-ALDRICH) were activated at 400 °C under vacuum for at least 3 hours.

Methanol, ethanol, n-butanol, toluene, n-pentane and THF (SIGMA-ALDRICH) were dried over activated molecular sieves 3Å (20 wt%) for a few days [57], then degassed by 3-times freeze-pump-thaw (standard procedure for ethanol, toluene, THF and n-pentane) or by argon flushing (at least 3 hours, for methanol and butanol).

Dichloromethane (VERBIESE) was dried over molecular sieves 3Å (20 wt%) for a few days, then degassed by 3-times freeze pumping.

All of these solvents were kept into closed Schlenk bottles under argon over molecular sieves.

CD_2Cl_2 (EUROSI-TOP, >99.8%) was dried over CaH_2 (SIGMA-ALDRICH), distilled under vacuum, degassed by 3-times freeze-pump-thaw and kept into an Mbraun glovebox under an atmosphere of purified nitrogen.

C_6D_6 (EUROSI-TOP, >99.8%) was dried over Na/K, distilled under vacuum, degassed by 3-times freeze-pump-thaw and kept into an Mbraun glovebox under an atmosphere of purified nitrogen.

$CDCl_3$ (EUROSI-TOP, >99.8%) was used as received.

Formaldehyde (SIGMA-ALDRICH, 37 wt% in H_2O containing 10-15% MeOH) was degassed by argon flushing and kept under argon into a closed Schlenk tube.

$P(OMe)_3$ (SIGMA-ALDRICH, >99%) was dried over molecular sieves 3Å (20 wt%), degassed by argon flushing, and kept into a closed Schlenk tube under argon atmosphere.

PMe_3 (SIGMA-ALDRICH, 1M solution in THF) was used as received.

PPh_3 (ALDRICH, >99%) was purified through crystallization in EtOH, and washed with glacial EtOH and pentane, then kept in a small Schlenk tube inside an Mbraun glovebox under an atmosphere of purified nitrogen.

Bis[(2-di-i-propylphosphino)ethyl]amine (PNP^HiPr, STREM CHEMICALS, 97%, 10 wt% solution in THF), $[RuCl_2(p\text{-cymene})]_2$ (STREM CHEMICALS, 10 wt% in THF), $NaBH_4$ (SIGMA-ALDRICH) and $NaHBEt_3$ (SIGMA-ALDRICH, 1M solution in toluene) were used as received, and kept into an Mbraun glovebox under an atmosphere of purified nitrogen.

3.2. Analytical instruments and methods

GC–FID/MS was carried out on Agilent 7890A (flame ionization detector) and Agilent 5975C (MS detector) instruments equipped with a Zeborn ZB-Bioethanol column (30 m column length ×0.25 mm internal diameter ×1.00 μm film thickness) with helium as carrier gas.

For GC-FID/MS analysis, the following oven temperature program was used:

50°C, 4 min;

then 5°C/min to 105°C

then 10°C/min to 200°C, then kept at 200°C for 3.5 minutes.

The total duration for this temperature program is 28 minutes.

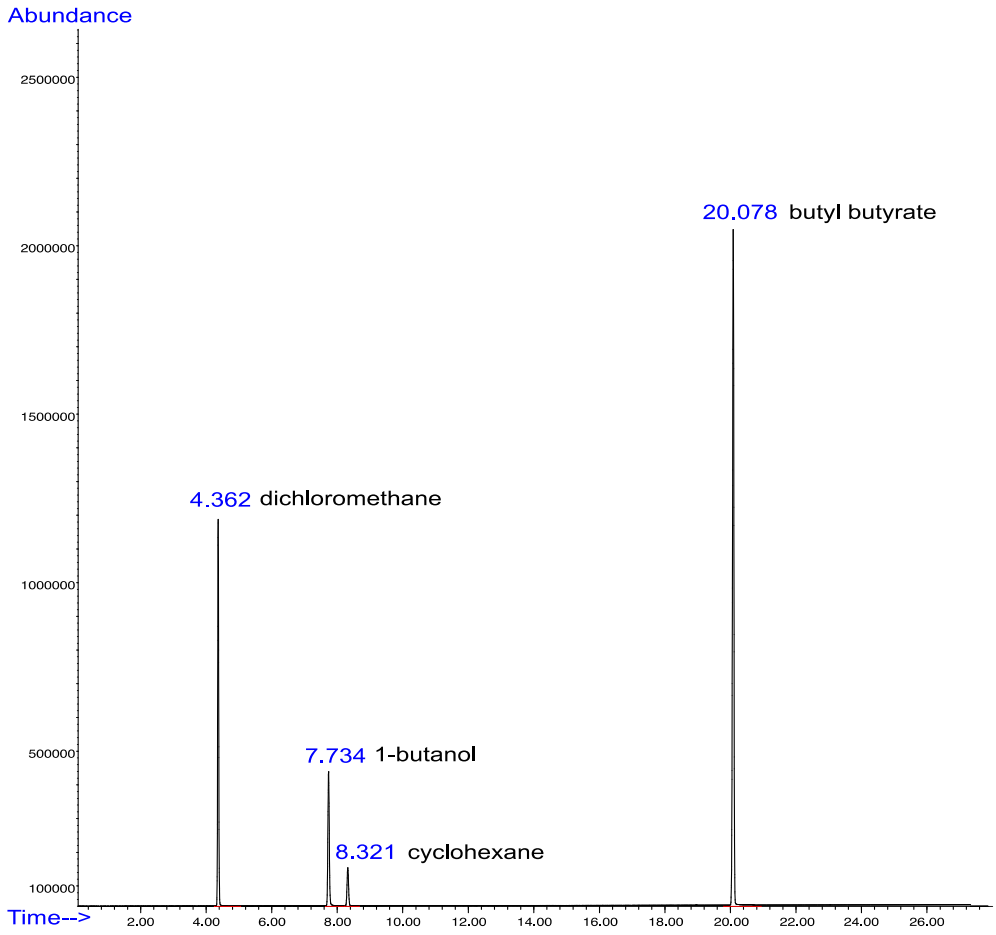

Figure 12. Typical FID chromatogram obtained for the acceptorless dehydrogenative coupling of butanol.

All ^{1}H-NMR and ^{31}P-NMR spectra were recorded on a Bruker Avance 300 NMR spectrometer and reported in ppm (δ).

About ^{1}H-NMR analysis for catalytic tests, it's possible to identify the signal of butanol at 3.6 ppm (CH_2 next to OH, triplet) and the one of ester at 4 ppm (CH_2 next to OR, triplet).

3.3. Standard procedure for catalytic test

3.3.1. Small volumes

3.3.1.a. Normal Schlenk tube

Inside a glovebox, the required amount of catalyst is weighted in a dried three-necked Schlenk tube fitted with a stirring bar (as large as possible) is put inside the glove box and filled with the amount of catalyst needed. The closed tube is then removed and put under vacuum (after 3 purges Argon/vacuum) to remove the glove box atmosphere, for a few minutes. Then the Schlenk tube is put under argon and fitted with the condenser topped with an argon bubbler, previously washed with acetone and dried with heating gun for about 20 minutes. The Schlenk bottle with butanol is also purged 3 times and left under argon to prevent air contamination during the withdrawal. The required amount of 1-butanol is taken via syringe (previously purged 3 times with Schlenk bottle's atmosphere), weighted before and after the loading, to have an accurate weight of the amount of reactant inside. When the tube is filled with the weighted reactant, it's put into the oil bath (previously heated at 130 °C), with the stirring rate set at 1050 rpm, to start the reaction. When the reflux starts, the first sample is taken out at reaction time zero.

3.3.1.b. Schlenk tube with baffles (tiny reactor)

Identical procedure is used. A small glass reactor fitted with baffles (breaking-vortex system) is utilized instead of a normal Schlenk tube. Stirring was provided by mechanical stirrer instead of a magnetic one. Stirring rate (ca. 1050 rpm) was kept the same as with the Schlenk tube.

3.3.2. Large volumes: big reactor

A Radley reactor ready 250 mL double walled with a bottom valve was used. The reactor is fitted with a Teflon impeller and Teflon baffles. The reactor lid ports are equipped with a reflux condenser topped with an argon bubbler, an argon inlet, an injection port closed with a septum and a dipping thermocouple. The reactor is heated and the reaction temperature monitored using a Huber Ministat 230 connected to the thermocouple dipped into the reaction mixture. Silicon oil is used as heating fluid. A Heidolph overhead mechanical stirrer is used for impeller rotation and accurate control of the stirring rate.

The reactor is preheated to 100°C under a gentle argon flow for 4h. In a glove box, the required amount of catalyst (typically 40 mg, 0.068 mmol) is weighed in a pressure equalising dropping funnel (custom built). Under argon, a first portion of 1-butanol (47.5 g) is introduced via syringe into the reactor. The reactor temperature set point is reduced to 80°C and the stirring is started at low stirring rate (100 rpm).

Under argon, the injection port (septum cap) is replaced by the pressure equalising dropping funnel containing the powered catalyst. Under argon, another portion of 1-butanol (15.6 g) is introduced via syringe into the dropping funnel to give a white suspension. The suspension is added into the reactor. The dropping funnel is rinsed with the last portion of 1-butanol (15.7 g) via syringe (1-butanol total = 78.8 g, 1.06 mol). At this point, the reaction media consist of a white-yellow suspension. The dropping funnel is replaced by a septum cap to allow for reaction sampling. The argon inlet flow is switched from the reactor lid to the bubbler topping the reflux condenser. The reaction temperature is set at 130°C and the stirring is set at the desired stirring rate (typically 1200 rpm). After 5 minutes, all the catalyst is dissolved (reaction temperature = ca. 90°C). After 15 minutes, reflux conditions are obtained (reaction temperature = 112°C). A first sample (typically 1 mL) is taken which corresponds to the reaction t_0.

3.4. Sampling method

Liquid samples (typically 0.2 ml) are taken out every 30 minutes for the first 2 hours with a standard 1 ml syringe (purged 3 times with reactor atmosphere before the withdrawal), then after 1 hour and finally every 2 hours, until the reaction is over (5, 7 or 9 hours, depending on the concentration of the catalyst). Every sample is analyzed by GC-FID/MS or by ^{1}H-NMR, to determine yield, turn over number, turn over frequency and conversion. The GC sample is composed by around 40 mg of crude product (weighted accurately) and 10-12

mg of internal standard (cyclohexane), then diluted with dichloromethane. The ^{1}H-NMR sample is composed by a few drops of crude product diluted with $CDCl_3$.

3.5. Complex synthesis

All the catalyst are synthesized in laboratory, except for Ru-MACHO-BH (Stream Chemistry, purity min. 98%). All the reactants and solvents are taken from the glove box (except for alcohols).

3.5.1. Synthesis of $RuHH(BH_3)(PNP^{H}iPr_2)PMe_3$

- step 0: synthesis of $[RuCl_2(PNP^{H}iPr_2)]_2$

0,505 g of $HN(CH_2CH_2PiPr_2)_2$ (10% w/w in THF, 1.64 mmol) is added to a suspension of $[RuCl_2(p\text{-cymene})]_2$ (500 mg, 0.81 mmol) in 20 mL THF. The solution is heated under reflux (oil bath, T=80°C, 1000 rpm) for 24 hours. during which a yellow precipitate is formed. The solvent is reduced under vacuum, and the residue is washed with 20 mL of pentane, and then removed using a syringe. The yellow powder product is dried under vacuum.

Yield: 0.655 g (0.741 mmol, 91.5%)

NMR: ^{1}H (CD_2Cl_2, 300MHz) δ = 6.22 ppm (s, N*H*); 3.17 – 2.99 (m, 2H, NCH_2); 2.88 – 2.71 (m, 2H, PC*H*$(CH_3)_2$); 2.65 – 2.44 (m, 2H, NCH_2); 2.15 – 2.01 (m, 2H, CH_2P); 2.01 – 1.91 (m, 2H, PC*H*$(CH_3)_2$); 1.51 – 1.41 (m, 6H, CH_3); 1.41 – 1.36 (m, 6H, CH_3);1.36 – 1.28 (m, 6H, CH_3); 1.24 – 1.16 (m, 6H, CH_3)

^{31}P [^{1}H] (CD_2Cl_2 ,121.5 MHz) δ= 78 (singlet)

(^{1}H and ^{31}P NMR spectra in agreement with literature data [58])

- step 1: synthesis of $[RuCl_2(PMe_3)(PNP^{H}iPr_2)]$

Under argon, $[RuCl_2(PNP^{H}iPr_2)]_2$ (0.2034 g, 0.23013 mol) is suspended in THF (5 mL) and PMe_3 (1M solution in THF, 0.503 mL) is added via syringe (very carefully, in contact with water it burns). The solution is stirred overnight, and then THF is removed under vacuum (1.10^{-3} mbar) at room temperature, to obtain an orange solid.

Yield: 0,2112 g (0,38159 mmol, 83%)

NMR: ^{31}P [^{1}H] (CD_2Cl_2 ,121 MHz) δ (PMe_3)= 7,1 (triplet); δ (PNP)= 40,3 (doublet)

- step 2: synthesis of [RuHH(BH_3)(PMe_3)(PNP^H*i*Pr_2)]

In a Schlenk tube under argon, [$RuCl_2$(PMe_3)(PNP^H*i*Pr_2)] (0.2112 g, 3.51 mmol) and $NaBH_4$ (0.171 g, 4.5 mmol) are dissolved in a mixture of toluene (13.5 mL) and ethanol (9.75 mL). The suspension is heated at 65 °C under stirring (900 rpm, closed Schlenk tube) for 3 hours. The solvents are removed under vacuum (1.10^{-3} mbar) at room temperature, to give a light yellow powder. This powder is diluted in CH_2Cl_2. The solution of dichloromethane and catalyst is filtered off, to separate NaCl and $NaBH_4$, and then the product is dried under vacuum (1.10^{-3} mbar) at room temperature.

Yield: 0.144 g (0,2889 mmol, 75.7%)

NMR: ^1H (CD_2Cl_2, 300MHz) δ (HBH_3)= -2.5 (multiplet); δ (Ru-H)= -17.6 (triplet)

^{31}P [^1H] (CD_2Cl_2 ,121.5 MHz) δ (PMe_3)= 10.3 (triplet); δ (PNP)= 68.6 (doublet)

3.5.2. Synthesis of RuHH(BH_3)(PNP^HiPr)P(OMe)$_3$

- step 1: synthesis of [$RuCl_2$P(OMe)$_3$(PNP^HiPr$_2$)]

P(OMe)$_3$ (23.3 mg, 0.1878 mmol) and dimer [$RuCl_2$(PNPHiPr)]$_2$ (75.6 mg, 0.08553 mmol) are dissolved in THF (6 mL). The viscous solution is stirred for 30 minutes (900 rpm) and a yellow precipitate is formed. THF is removed under vacuum (1.10^{-3} mbar) at room temperature and the precipitate is washed with pentane (2 x 3 mL), then dried under vacuum (1.10^{-3} mbar) at room temperature, to obtain a white powder.

Yield: 0.091 g (0.151 mmol, 88.3%)

NMR: ^{31}P [^1H] (CD_2Cl_2 ,121.5 MHz) δ (P(OMe)$_3$)=135 (triplet); δ (PNP)=39 (doublet)

- step 2: synthesis of [RuHH(BH_3)P(OMe)$_3$(PNP^HiPr$_2$)]

Under argon, in a dried Schlenk tube, $NaBH_4$ (0.0654 g, 1.729 mmol) and [$RuCl_2$P(OMe)$_3$(PNP^H)] (0.091 g, 0.151 mmol) are suspended in a mixture of toluene (5.2 mL) and ethanol (3.9 mL). The suspension is heated at 65°C and stirred (900 rpm) for 3.5 hours. Solvents are then removed under vacuum to obtain a white powder. The solid is dissolved in CH_2Cl_2 and the solution is filtered off, to separate solid NaCl and $NaBH_4$ residual. Dichloromethane is removed under vacuum and the product is finally washed with pentane (3 x 4 mL), to obtain an off-white powder.

Yield: 0.0778 g (0.142 mmol, 94.1%)

NMR: ^1H (CD_2Cl_2, 300MHz) δ (HBH_3)= -2.5; δ (Ru-H)= -15.7 (triplet)

traces of impurities at -19.7ppm (<10%)

^{31}P [^1H] (CD_2Cl_2 ,121.5 MHz) δ (P(OMe)$_3$)= 178 (triplet); δ (PNP)= 69.8 (doublet)

traces of impurities at 65.1ppm (<10%)

3.5.3. Synthesis of [$RuHCl(CO)(PPh_3)_3$]

This synthesis is largely described in literature [59].

In a glovebox, PPh_3 (0.220 g, 0.830 mmol) is weighted in a Schlenk tube containing a stirring bar. Under argon, MeOH (20 mL) is added, the tube is equipped with a condenser and the suspension is refluxed until all the phosphine solubilizes (ca. 20 min). Meanwhile, under argon, $RuCl_3{*}H_2O$ (0.0356 g, 0.152 mmol) is weighted in a Schlenk tube and suspended in methanol (4 mL). Under argon,the PPh_3 solution is added to the $RuCl_3$ solution via cannula. Then HCHO (37% mol solution, 4 mL, previously degassed) is quickly added into the Schlenk via syringe. The color changes from red to dark green. The resulting solution is left refluxing for 2 hours.

The system is then cooled down using an ice bath under magnetic stirring for around 30 minutes. The liquid part is filtered-off and the precipitate is washed twice with pentane (2 x 5 mL). The resulting solid product is dried under vacuum overnight (1.10^{-3} mbar) at room temperature.

Now the product is further washed with ethanol (5 ml), water (5 ml, previously degassed), ethanol (5 ml) and pentane (5 ml). The product is dissolved in toluene (ca. 4 ml) and filtered over activated Al_2O_3. Finally, toluene is removed under vacuum, and the product is washed with pentane (2 x 4 mL) to obtain a white powder.

Yield: 0.120 g (0.126 mmol, 83%)

NMR: ^1H (C_6D_6 300MHz) δ (hydride)= -7,5 (triplet);

^1H and ^{31}P NMR spectra in agreement with literature data [63].

3.5.4. Synthesis of [$RuHClCO(PNP^HiPr_2)$]

In a glovebox, [$RuHCl(CO)(PPh_3)_3$] (0.999 g, 1.042 mmol) and PNP^HiPr_2 (10 wt% in THF, 3.600 g, 1.179 mmol, 1.12 equiv) are weighted in a Schlenk tube. THF is removed under vacuum and diglyme (4 mL) is added to form a suspension. Under argon, the tube is dipped in an oil bath preheated at 165 °C, and stirred magnetically for 90 minutes. During this period the suspension changes color: from the initial beige to a light green, then it turns yellow. At this point the tube is cooled into a freezer inside the glovebox (-22°C) for around 2 hours. After this time, a white precipitate is formed. The liquid part is then removed using a syringe, and the white precipitate is washed with diethyl ether (3 x 4 mL) and finally dried under vacuum (1.10^{-3} mbar) at room temperature to obtain a white powder.

Yield: 0.403 g (0.856 mmol, 82%)
NMR: ^{31}P [^{1}H] (CD_2Cl_2) δ= 74.8 (singlet), pur.>98% (^{1}H and ^{31}P NMR spectra in agreement with literature data [60])

3.5.5. Synthesis of $RuH(OCOCH_3)CO(PNP^{H}iPr_2)$

In a glove box, [$RuHClCO(PNP^{H}iPr_2)$] (0.103 g, 0.2187 mmol) and CH_3COOAg (0.0446 g, 0.2672 mmol) are weighted in a Schlenk tube and suspended in toluene (2 mL). The suspension is stirred overnight at room temperature. The resulting mixture is filtered over a silica pad, to remove the excess of silver acetate and washed with toluene (2 ml). The solvent is removed under vacuum and the product is dissolved in pentane (2 x 4 mL). This brown solution is filtered again via syringe (2 times). The obtained colorless solution is dried under vacuum and the product is obtained as a white powder.
Yield: 0.0778 mg (0.1233 mmol, 72.7%)
NMR: ^{1}H (C_6D_6 300MHz) δ (Ru-H)= -18 (triplet)
^{31}P [^{1}H] (C_6D_6 121.5 MHz) δ= 89.9 (singlet)

3.5.6. Synthesis of $[RuH_2(CO)(PNP^{H}iPr_2)]$

In a glove box, [$RuHClCO(PNP^{H}iPr_2)$] (0.221 g 0.468 mmol) is weighted into a Schlenk tube and dissolved in THF (8 mL), then $NaHBEt_3$ is added (0.45 ml, 1M solution in THF, 0.45 mmol, 0.96 equiv). The solution is stirred at room temperature into the glovebox overnight, and it slowly becomes yellow. THF is removed under vacuum, and the yellow wet powder is washed with toluene (6-8 ml) and filtered off. Finally toluene is removed under reduced pressure (dihydride is quite unstable under vacuum) and the product is washed with pentane, to give a light yellow powder.
Yield: 0,182 g (0,417 mmol, 89,1%)
NMR: ^{1}H (C_6D_6 300MHz) δ = 2.20 – 2.04 (m, 3H); 1.92 – 1.83 (m, 4H); 1.66 – 1.54 (m, 2H); 1.36 – 1.27 (m, 24H); 1.01 – 0.91 (m, 2H); -6.18 - -6.46 (m, RuH_2)
^{31}P [^{1}H] (C_6D_6 121.5 MHz) δ = 91.1 ppm (singlet, PNP)
(^{1}H and ^{31}P NMR spectra in agreement with literature data [60])

3.5.7. Synthesis of [RuHH(BH_3)(CO)($PNP^H iPr_2$)]

In a glovebox, [RuHClCO($PNP^H iPr_2$)] (0.195 g, 0.414 mmol) and $NaBH_4$ (0.160 g, 4.229 mmol, 10.2 equiv) are weighted in a dried Schlenk tube, and toluene (16 mL) is added via syringe. Then of ethanol (12 mL) is added under argon and the solution is heated (65 °C) and stirred for four hours.

Yield: 0.169 g (0.376 mmol, 90.5%)

NMR: ^1H (CD_2Cl_2, 300MHz) δ = 3.90 ppm (large, N*H*); 3.30 – 3.12 (m, 2H); 2.56 – 2.44 (m, 2H); 2.30 – 2.21 (m, 2H); 1.94 – 1.82 (m, 2H); 1.38 (dd, J_{HP} = 16,4Hz, J_{HH} = 7,5Hz; 6H); -1.92 - -2.69 (large, *H*B*H*$_4$); -13.53 ppm (J_{HP} = 17,1Hz; Ru*H*)

^{31}P [^1H] (CD_2Cl_2, 121.5 MHz) δ = 77.7 ppm.

4. Results and discussion

4.1. Reactor type

Evaluation of diffusive regimes and kinetic limitations due to mass transfer (evolution of molecular hydrogen), but also of any problem arising from an increase in the volume (first steps towards an industrial scale-up), requires a preliminary discussion about the right type of reactor to use.

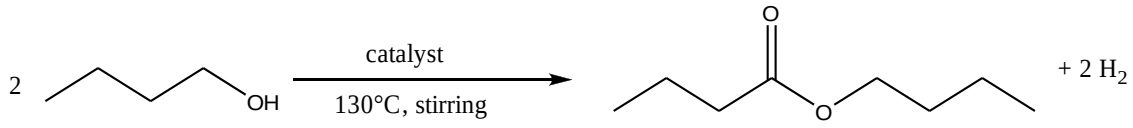

Scheme 15. Acceptorless dehydrogenative coupling of 1-butanol to butyl butyrate.

As mentioned above, evaporation of molecular hydrogen seems to affect the smooth progress of the reaction. In fact, for every mole of butyl butyrate formed, two moles of H_2 are generated. If the reaction system cannot properly remove the hydrogen liberated, the conversion and yield could be strongly influenced by the possible, concomitant reverse reduction reaction.

The conditions to ensure an effective disposal of the generated gas can be reached by working at reflux, in an open system, under vigorous stirring, inside a reactor where the contact surface is great enough to ensure efficient mass transfer. Therefore, the reactor must be equipped with a stirring system (magnetic or mechanical) and with a condenser. The option of an open-air condenser system compared to a controlled atmosphere apparatus has to be evaluated, because the catalysts are very oxygen-sensitive. This fact can strongly influence the characteristics of the reactor, which could have to guarantee minimal external contaminations through an inert-gas fluxing system.

4.1.1 Normal Schlenk tube

A typical, widely used reaction vessel in air sensitive chemistry is the Schlenk flask, or Schlenk tube. Therefore, the efficacy of a normal three-necked Schlenk tube was firstly analyzed. The tube was fitted with a condenser and topped with an argon bubbler (to minimize the risk of external contact). The benefits of this type of reactor are correlated to its characteristics: its small size allows easy access inside the glovebox where the air

sensitive catalyst can be stored without any risk of contaminations; the glovebox atmosphere (sometimes full of volatile compounds) could be removed under vacuum; the reaction could run without interferences. Anyway, the main problem arising from the use of a normal Schlenk tube lies in its round bottomed shape: under stirring, this leads to the formation of a vortex that may not provide an effective contact surface for hydrogen evolution. Indeed, to maximize this surface, the stirring bar inside the tube has to be as large as possible.

4.1.2. Schlenk tube with baffles (Tiny reactor)

Figure 13. Tiny reactor with magnetic stirring system (first version, not used).

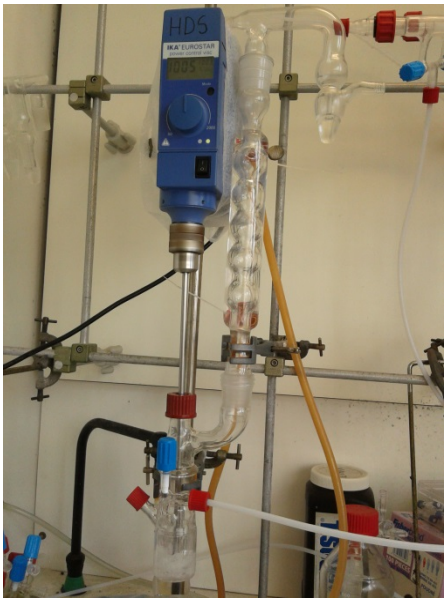

Figure 14. Tiny reactor with mechanical stirring system.

A normal Schlenk tube is equipped with baffles in order to break the vortex formed at high stirring rate, hence increasing the amount of hydrogen released by maximizing interface area. To make the contact surface as large as possible two stirring systems were investigated: magnetic and mechanical. However, magnetic stirring immediately proved to be ineffective, because of the tendency of the stir bar to slam against the baffles, leading to momentarily interruptions of agitation (and hence non-reproducible results), as well as the rupture of the glass deflectors themselves. Therefore, all the reported results were obtained under mechanical stirring.

This small reactor equipped with mechanical stirring (tiny reactor) has all the benefits of a normal Schlenk tube, but its different frame could lead to contamination problems during the assembly. In fact, it is composed by two different pieces: the reactor itself (lockable with a cap) and the apparatus condenser-mechanical stirrer, which has to be

perfectly aligned to the reactor prior to start the reaction under controlled atmosphere, Alignment of the apparatus is a crucial point to avoid slamming of the impeller onto the baffles and is also related to results reproducibility. Of course, the more time is dedicated to reactor assembly, the higher is the risk of contamination of the reaction vessel.

4.1.3. Big reactor

Figure 15. Big reactor.

This reaction system is totally different from the others. Its total volume is 250 ml (normally filled with 100 ml, i.e. about five time more than a normal Schlenk tube), its main structure is not-movable, but it is overall composed by many different pieces: condenser, internal thermometer, internal oil bath, teflon baffle, movable piece of glassware to load the catalyst inside the glove box. This could lead to problems in applying vacuum to the reactor and hence to possible contaminations from the glovebox atmosphere and drying problems. The temperature inside the reactor is continuously monitored by the internal thermometer, which directly transfers the data to an external computer. This computer regulates the temperature of the internal oil bath and monitors the internal temperature of the reactor.

On one side, this reaction system is very useful to test reactions on a bigger scale, provides an accurate control on the internal temperature, and the mechanical stirring system could reach very high stirring rate (up to 1800 rpm) that, combined with the baffle-system and the open-air condenser, can dispose hydrogen in a very efficient way. On the other side, all the movable parts make it easily affected by external contaminations, especially when it is loaded with low amounts of catalyst (that implies longer reaction times).

4.2. Catalyst structure/reactivity

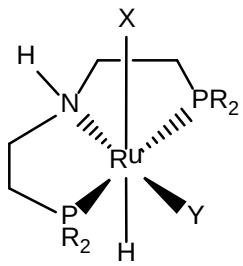

Ru-MACHO-BH : R = Ph; X = HBH_3; Y = CO;
1a : R = *i*Pr; X = HBH_3; Y = CO;
1b : R = *i*Pr; X = H; Y = CO;
2a : R = *i*Pr; X = HBH_3; Y = $P(CH_3)_3$;
2b : R = *i*Pr; X = HBH_3; Y = $P(OCH_3)_3$.

Figure 16. General structure of catalysts tested.

Both *in situ* formed and isolated ruthenium complexes were studied as catalysts for the dehydrogenative coupling of 1-butanol.

As previously mentioned, the most known and used commercial catalyst for this type of reaction is Ru-MACHO-BH (Takasago Fine Chemical Division). Starting from this very expensive complex, a series of catalytic tests was conducted, in order to establish:

1. the right concentration of catalyst, which allows for a correct reaction kinetics (not influenced by mass transfer of molecular hydrogen in the gas phase), thus ensuring good values of yield, conversion, turnover number (TON), and turnover frequency (TOF);

2. the best reaction system, that can maximize catalyst's performance by guaranteeing an effective disposal of the generated hydrogen and minimisation of external contaminations;

3. the best catalyst, in terms of catalytic performance, resistance to deactivation, and cost.

4.2.1. Catalysts tested

To evaluate the influence of the different ligands on catalytic performance, a series of different catalysts is tested. All catalysts listed below were synthesized in the laboratory (see "Complex Synthesis", Experimental Part), except for Ru-MACHO-BH.

Isolated catalyst:

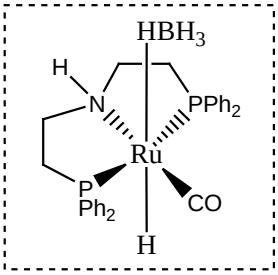

Ru-MACHO-BH (Stream Chemicals)

In situ formed catalysts:

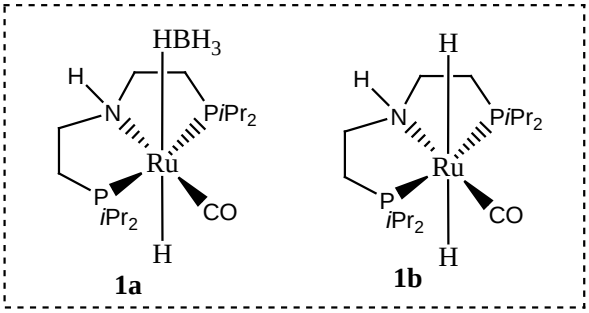

New formed catalyst:

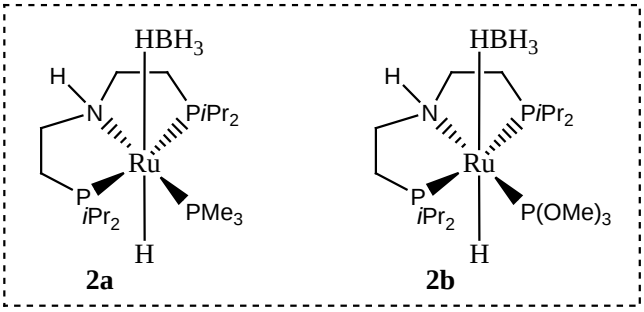

Figure 17. Catalysts tested for dehydrogenative coupling of butanol to butyl butyrate.

Molecular weights:

- **Ru-MACHO-BH** = 586.27 g/mol
- **1a** = 450.36 g/mol
- **1b** = 436.52 g/mol
- **2a** = 498.43 g/mol
- **2b** = 601.47 g/mol

All complexes were found to have a purity higher than 98% (as deduced from ^{31}P [^{1}H decoupled] NMR spectra).

4.2.2. Catalytic tests

All the analysis performed on different catalysts, at different concentrations, and in different reactors are reported below. For each test, results are shown as graphs related to yields, TON, and initial TOF, to express qualitatively the progress of the reaction, and then reported into tables, with the values related to conversion, yield, TON, and TOF, for a quantitative assessment of catalyst activity and productivity. For each catalyst concentration the tests are duplicated to ensure reproducibility and accurate measurement of the reaction rate, expressed as the initial turnover frequency (TOF_0).
Common abbreviations used to describe reactor's type: S.T., Schlenk tube; B.R., Big reactor; T.R., Tiny reactor (Schlenk tube with baffles).

4.2.2.1. Isolated catalyst : Ru-MACHO-BH

The catalytic performance of the commercial **Ru-MACHO-BH** (Stream Chemicals) was first examined.
A series of tests was conducted at different catalyst loadings in all three reactors.

Table 4. Overview of different tests on Ru-MACHO-BH. (F) = failed experiment

Reactor / Concentration	**S.T.**	**B.R.**	**T.R.**
250 ppm	X X	X X	X X
100 ppm	X X (F)		X X (F)
60 ppm	X X (F)	X X	
20 ppm	(F)	X X (F)(F)	(F)

Non-reproducible data deriving from failed experiments were commonly obtained. The reasons are mainly connected to oxygen contamination (arrest of the argon flow, leak in the system, reactants not sufficiently degassed, glassware not enough dried, etc.) or problems related to the stirring system (stir bar too small, arrest of mechanic system).
The reported tests are not affected from this kind of problems.

A. Schlenk tube

The following tests were conducted in a normal Schlenk tube, using n-butanol as substrate.

Table 5. Catalytic tests carried into Schenk tubes at different concentrations of Ru-MACHO-BH.

entry	**m tot cat (g)**	**m tot BuOH (g)**	**n tot cat (mol)**	**n tot BuOH (mol)**	**ppm tot cat**	**ID**
S.T.- 1	0,016	8,066	2,7291E-05	0,108823529	250,78381	S.T.-251ppm
S.T.- 2	0,0165	8,067	2,8144E-05	0,108837021	258,58875	S.T.-258ppm
S.T.- 3	0,0171	20,0803	2,9167E-05	0,270916082	107,6623	S.T.-108ppm
S.T.- 4	0,0161	20,4756	2,7462E-05	0,276249325	99,409291	S.T.-99ppm
S.T.- 5	0,0078	16,3347	1,3304E-05	0,220381813	60,37	S.T.-60ppm
S.T.- 6	0,0081	16,2033	1,3816E-05	0,218609012	63,200321	S.T.-63ppm

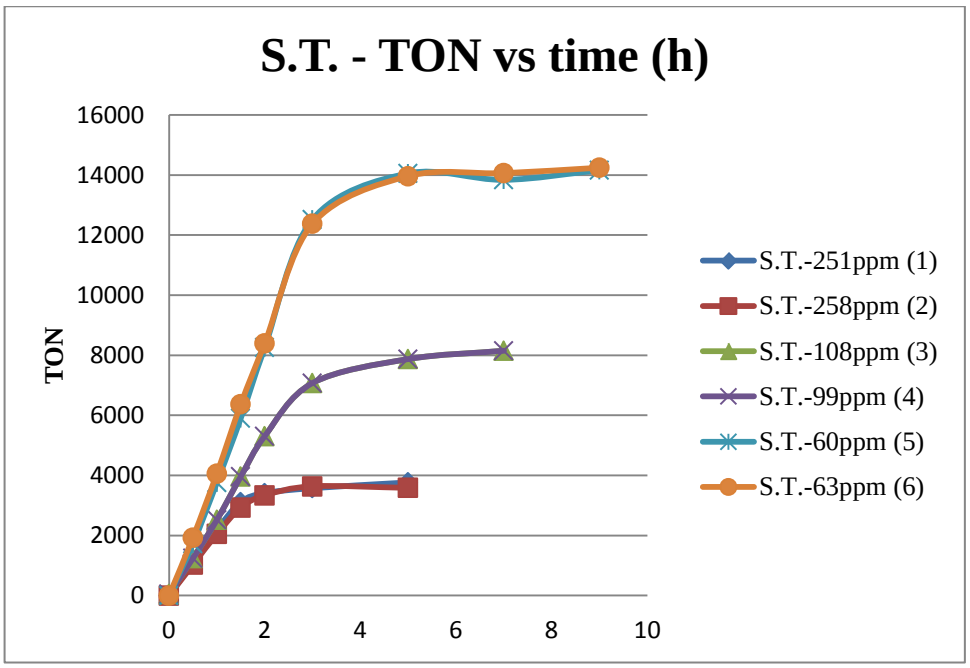

Graphic 1. TON vs time (h). Schlenk tube, different catalyst loading.

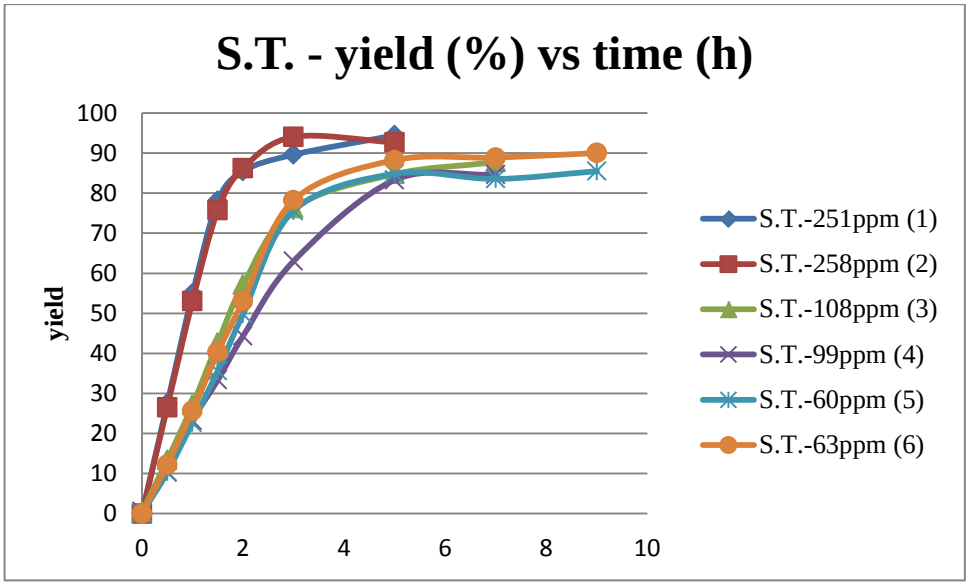

Graphic 2. Yield (%) vs time (h). Schlenk tube, different catalyst loading.

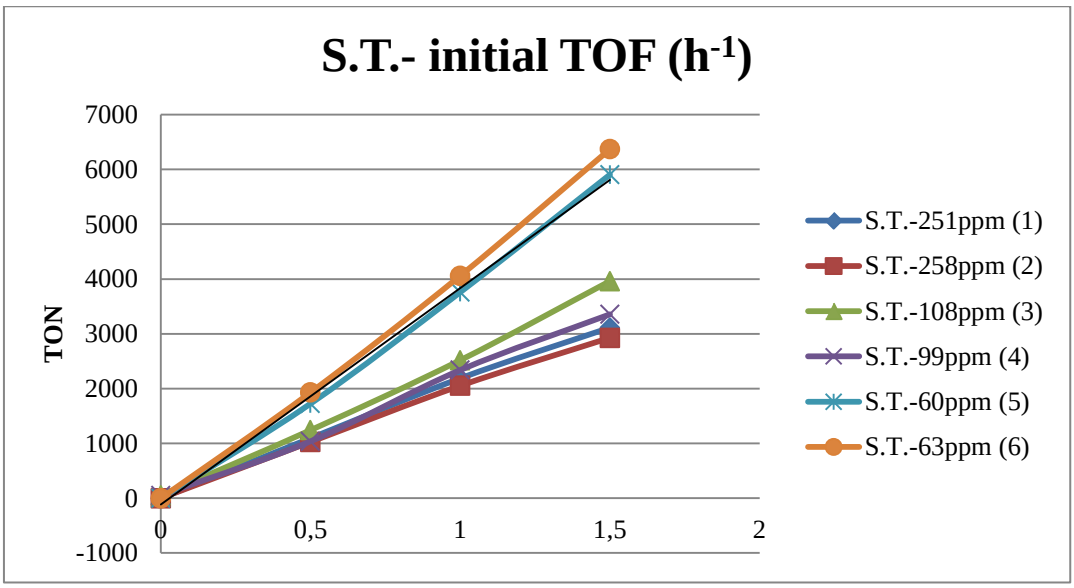

Graphic 3. Initial rate of reactions.

Table 6. Experimental data for Ru-MACHO-BH at different concentrations.

entry	max Conversion (%)	max Yield (%)	max TON	initial TOF (h^{-1})
S.T.-251ppm (1)	95,6 (after 5 h)	94,4 (after 5 h)	3766 (after 5 h)	2188
S.T.-258ppm (2)	95,7 (after 5 h)	92,7 (after 5 h)	3584 (after 5 h)	2052
S.T.-108ppm (3)	89,4 (after 7 h)	87,7 (after 7 h)	8149 (after 7 h)	2466
S.T.-99ppm (4)	87,1 (after 7 h)	84,6 (after 7 h)	8512 (after 7 h)	2285
S.T.-60ppm (5)	87,9 (after 7 h)	85,5 (after 9 h)	14159 (after 9 h)	4228
S.T.-63ppm (6)	91,0 (after 9 h)	90,0 (after 9 h)	14244 (after 9 h)	4170

Catalyst: **Ru-MACHO-BH**; substrate: n-butanol; applied temperature: 130°C; under argon

Discussions

Duplication of reactions has ensured excellent reproducibility (see Graphs 1, 2 and 3).

All the investigated loadings were found to be very active, with minimal final conversion and yield of 87.1 % and 84.6%, respectively (see entry 4, Table 6).

Unexpectedly, a decrease in catalyst concentration does not correspond to a clear decrease in its activity. For 250 ppm catalyst loading, maximum yields and conversions are reached (entry 1 and 2, Table 6) and the reaction is exhausted in less than 3 hours, while for 60 ppm concentration, the reaction has a regular pattern for around 5 hours (Graphic 2). This means that the reaction system (Schlenk tube) is very suitable for ensuring lack of external contaminations, also for long reaction times (at 60 ppm the reaction was investigated for 9 hours).

As described in the literature, expressing TON as a function of time for different catalyst concentrations (Graphic 3) one can observe that the lowest catalyst loading led to the most active catalytic system, with higher TOF_0. This suggests that the overall reaction kinetics is not first order relative to catalyst concentration, since this would lead to TOF_0 independent to its loading. This fact could be explainable if one considers mass transfer of hydrogen in the gas phase. Indeed, for 250 ppm catalyst loading the reaction system may not be as effective in the disposal of hydrogen (massive hydrogen evolution) as for 60 ppm (less hydrogen generated). This hypothesis has to be proved by investigating other reaction systems.

B. Big reactor

The following tests were conducted into a big reactor system (previously described).

Table 7. Catalytic tests carried into big reactor at different concentrations of Ru-MACHO-BH.

entry	**m tot cat (g)**	**m tot BuOH (g)**	**n tot cat (mol)**	**n tot BuOH (mol)**	**ppm tot cat**	**ID**
B.R.- 1	0,1594	81,3226	0,000271888	1,097174852	247,8077	B.R. - 247ppm
B.R.- 2	0,1592	81,1265	0,000271547	1,094529142	248,09503	B.R. - 248ppm
B.R.- 3	0,03917	80,4401	6,68122E-05	1,085268484	61,562849	B.R. - 62ppm
B.R.- 4	0,0389	80,7162	6,63517E-05	1,088993524	60,929362	B.R. - 61ppm
B.R.- 5	0,0139	80,8565	2,37092E-05	1,0908864	21,733897	B.R. - 21ppm
B.R.- 6	0,0141	80,7633	2,40504E-05	1,08962898	22,072056	B.R. - 22ppm

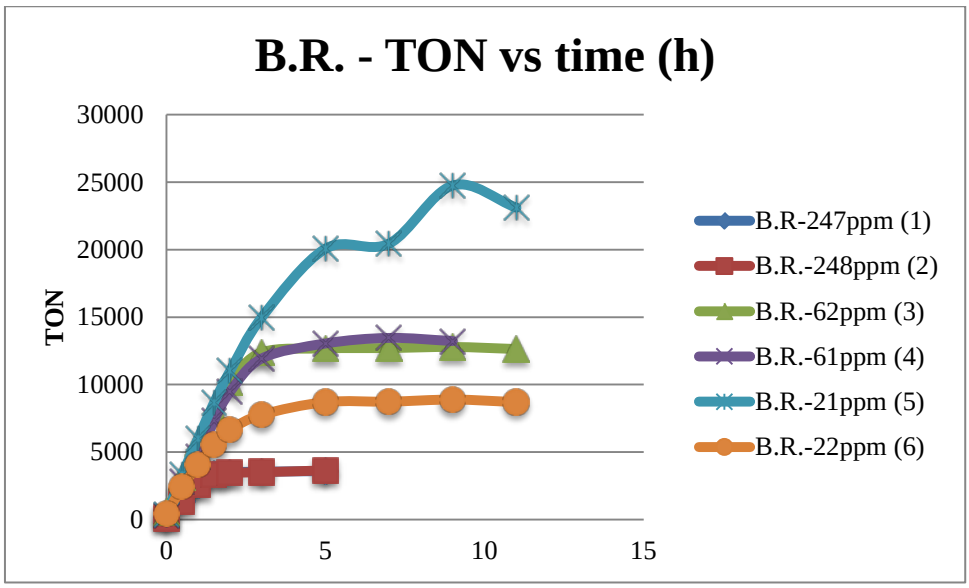

Graphic 4. TON vs time (h). Big reactor, different catalyst loading

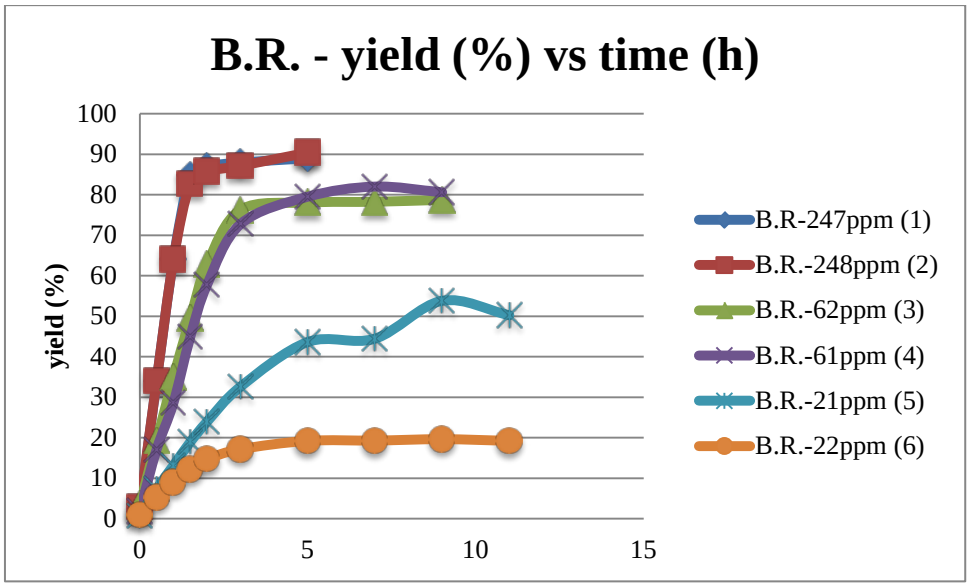

Graphic 5. Yield (%) vs time (h). Big reactor, different catalyst loading.

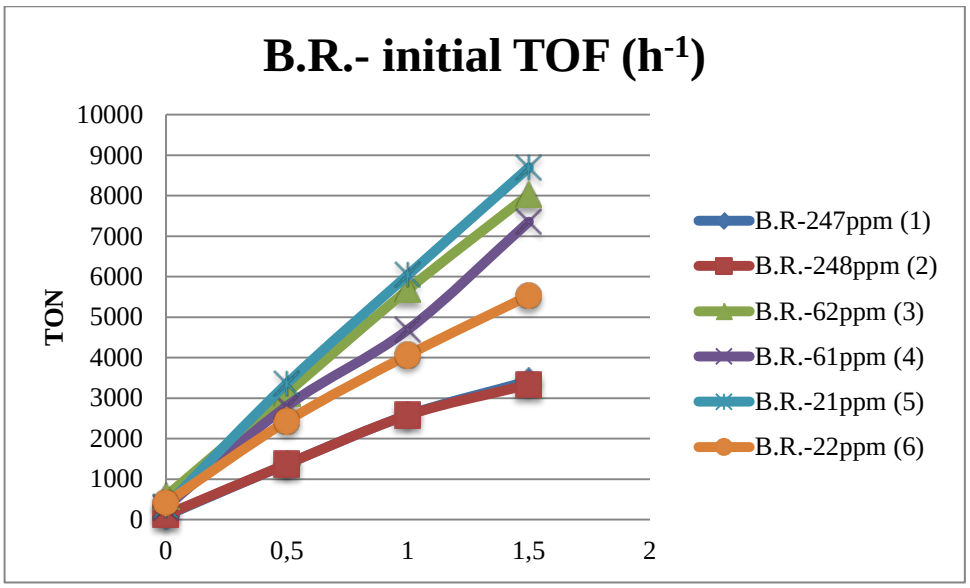

Graphic 6. Initial rate of reactions.

Table 8. Experimental data for Ru-MACHO-BH at different concentrations.

entry	max Conversion (%)	max Yield (%)	max TON	initial TOF (h^{-1})
B.R. - 247ppm (1)	91,6 (after 5 h)	89 (after 5 h)	3591 (after 5 h)	2490
B.R. - 248ppm (2)	90,8 (after 5 h)	90,4 (after 5 h)	3643 (after 5 h)	2459
B.R. - 62ppm (3)	81,9 (after 7 h)	78,7 (after 9 h)	12788 (after 9 h)	4826
B.R. - 61ppm (4)	83,1 (after 9 h)	82,1 (after 7 h)	13228 (after 9 h)	4578
B.R. - 21ppm (5)	44,9 (after 9 h)	53,8 (after 9 h)	22064 (after 11 h)	5550
B.R. - 22ppm (6)	20,8 (after 11 h)	19,6 (after 9 h)	8704 (after 11 h)	3397

Catalyst: **Ru-MACHO-BH**; substrate: n-butanol; applied temperature: 130°C; under argon

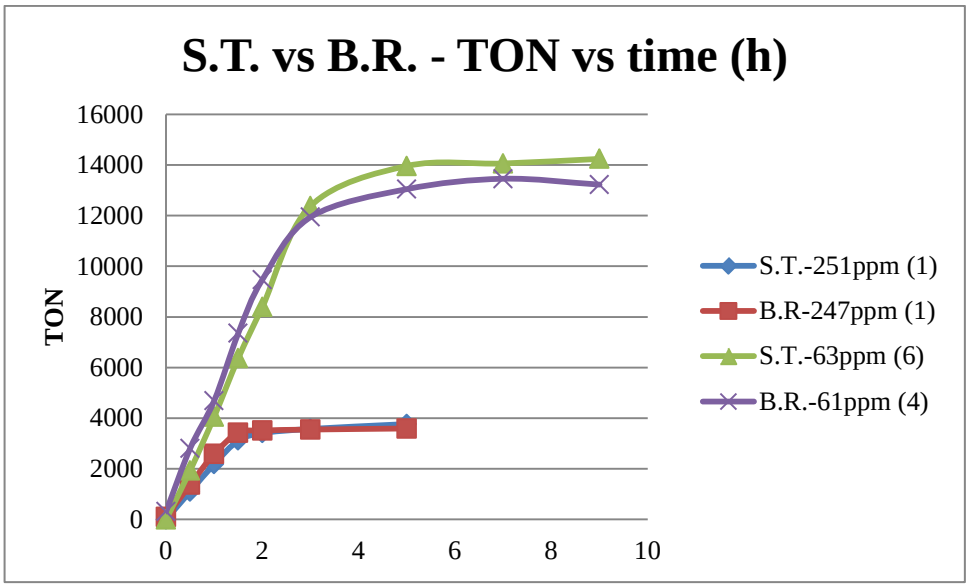

Graphic 7. Performance comparison between big reactor and Schlenk tubes.

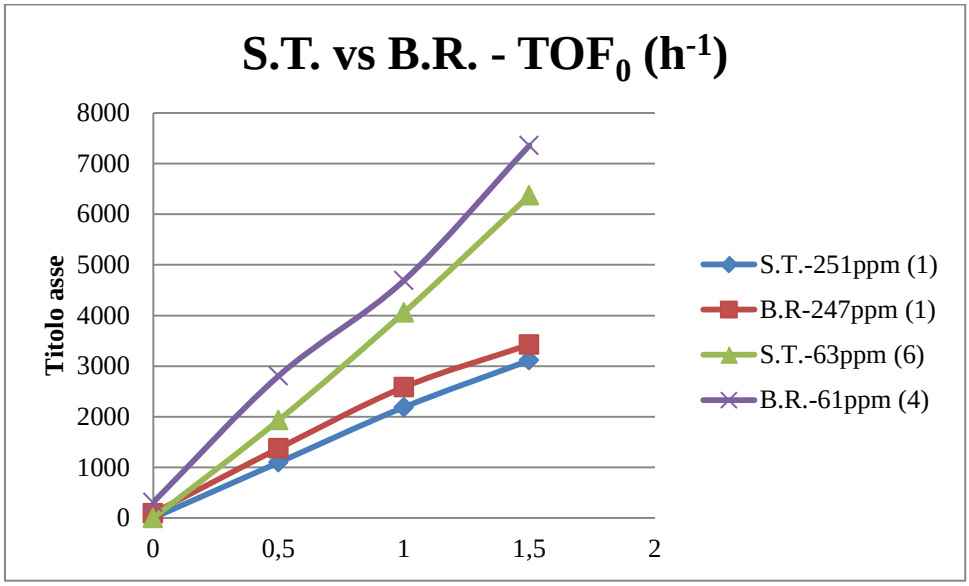

Graphic 8. Initial reaction rate: comparison between the two systems.

Discussions

Results reproducibility is observed for catalyst concentrations higher than 20 ppm (see Graphic 4 and 5). This time, a decrease in catalyst concentration leads, as expected, to a decrease of the general productivity. The best results in terms of yield and conversion were obtained for 250 ppm catalyst loading (see entry 1 and 2, Table 8). In general, trend and results are comparable to those obtained into the Schlenk tubes (see Graphic 7), although the values are lower for lower concentrations (see entry 3 and 4, Table 8 and Graphic 7).

For 20 ppm catalyst loading, the worst results in terms of yields and conversion were obtained, but also the highest TOF_0 was recorded. Even if the analysis was not reproducible, both tests conducted at this concentration showed better values of TOF_0 than those conducted at 250 ppm (see entry 5 and 6 Table 8, and Graphic 6).

Some considerations can be drawn from these results:

- the Schlenk tube is a better system to avoid external contaminations (best values of conversion and yield even for long times of analysis);
- for catalyst loading lower than 60 ppm the initial reaction rate is higher but the catalyst could be easily deactivated, especially in big reaction systems;
- the reaction rate seems to be influenced by hydrogen diffusion;

- the big reactor is not usable for long reaction times, although it guarantees a better disposal of generated hydrogen, even for high concentrations of catalyst (see Graphic 8);

It is therefore necessary to find a reaction system which could combine the capability of hydrogen disposal of the big reactor with the reliability and reproducibility of the Schlenk tubes.

C. Tiny reactor

Table 9. Catalytic tests conducted into Tiny reactor at different concentrations of Ru-MACHO-BH.

entry	m tot cat (g)	m tot BuOH (g)	n tot cat (mol)	n tot BuOH (mol)	ppm tot cat	ID
T.R.- 1	0,0336	16,1686	5,73115E-05	0,218140853	262,7269351	T.R. - 262ppm
T.R.- 2	0,0334	16,1815	5,69703E-05	0,218314895	260,9548834	T.R. - 260ppm
T.R.- 3	0,03917	80,4401	6,68122E-05	1,085268484	61,56284886	T.R. - 102ppm
T.R.- 4	0,0389	80,7162	6,63517E-05	1,088993524	60,9293623	T.R. - 105ppm

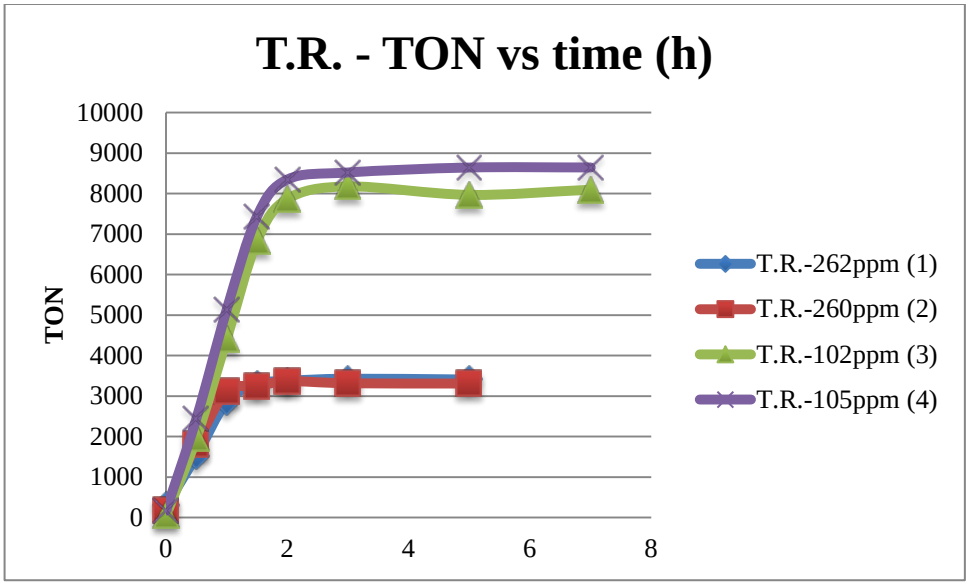

Graphic 9. TON vs time (h). Tiny reactor, different catalyst loading.

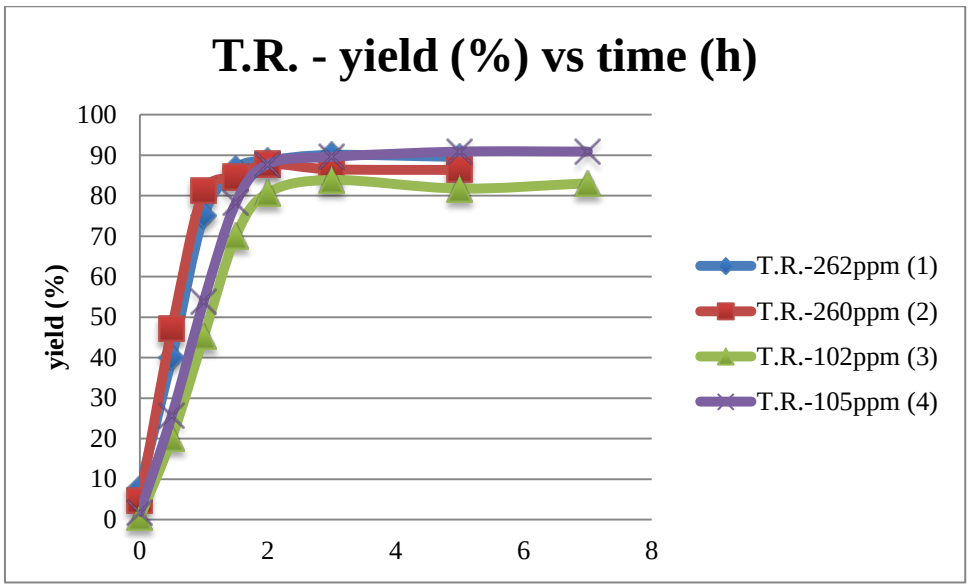

Graphic 10. Yield (%) vs time (h). Tiny reactor, different catalyst loading.

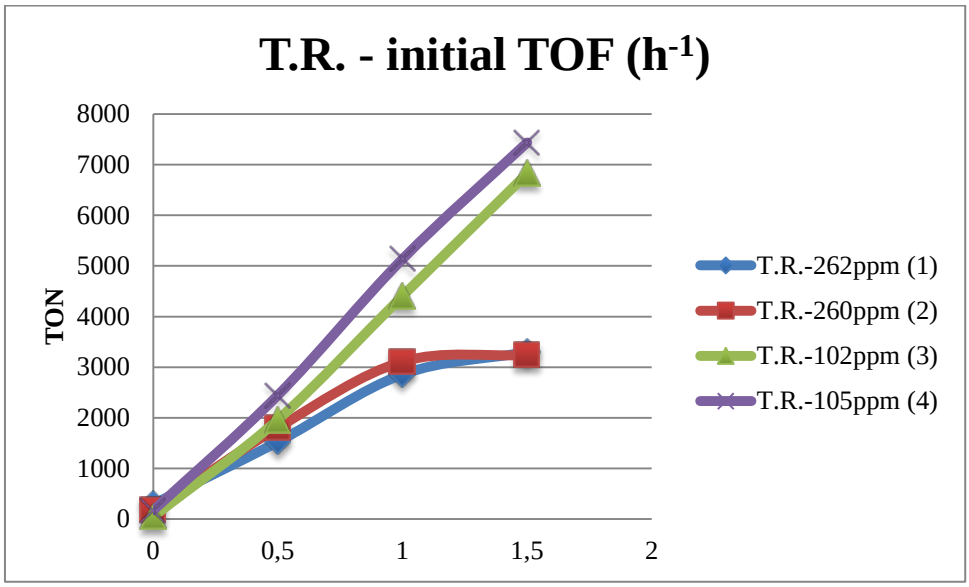

Graphic 11. Initial rate of reactions.

Table 10. Experimental data for Ru-MACHO-BH at different concentrations.

entry	max Conversion (%)	max Yield (%)	max TON	initial TOF (h^{-1})
T.R. - 262ppm (1)	93,6 (after 5 h)	90,1 (after 3 h)	3428 (after 3 h)	2564
T.R. - 260ppm (2)	90,5 (after 3 h)	87,8 (after 2 h)	3365 (after 2 h)	2929
T.R. - 102ppm (3)	91,7 (after 3 h)	83,9 (after 3 h)	8176 (after 3 h)	4966
T.R. - 105ppm (4)	95,2 (after 3 h)	90,9 (after 7 h)	8644 (after 7 h)	4358

Catalyst: **Ru-MACHO-BH**; substrate: n-butanol; applied temperature: 130°C; under argon

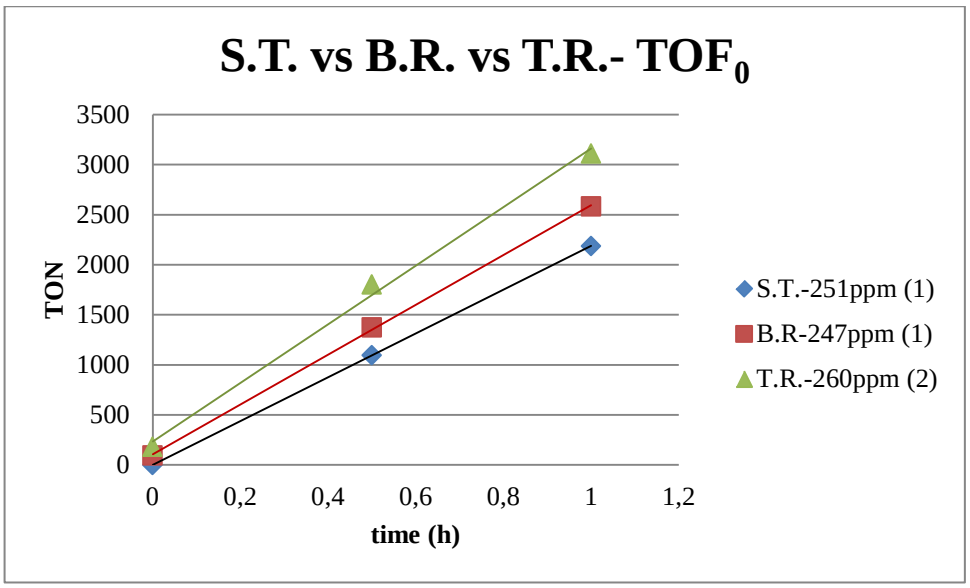

Graphic 12. Comparison between different reactors: reaction rates.

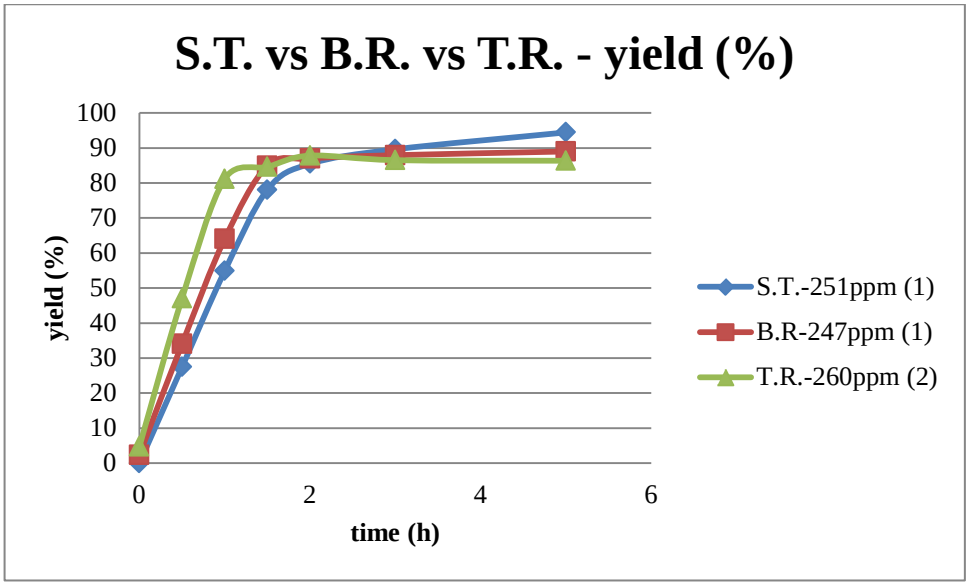

Graphic 13. Comparison between different reactors: yields.

Discussions:

This type of reactor guarantees reproducibility of the results and optimal values of yields and TONs, also with 100 ppm catalyst loading (see Graphic 9 and 10 and Table 10). The best catalytic activity was obtained for 105 ppm catalyst loading, with maximum conversion of 95.2% and maximum yield of 90.9 % (Table 10, entry 4).

In general, the reactions carried out into this tiny reactor seem to be faster than those conducted into the other two systems (see Graphic 12), with a maximum TOF_0 of 4966 h^{-1}, the highest ever recorded so far (see Table 10 entry 3). This means that this system is the best in terms of catalytic activity (conversion, yield and TON) and hydrogen disposal (TOF_0).

It can also be notice that a catalyst concentration of 100 ppm guarantees optimal values of catalytic activity and reaction rate, that appears not to be influenced by hydrogen diffusion.

4.2.2.2. In situ *and new formed catalysts*

After the investigation on the efficiency of the reactors and the effect of catalyst concentration on the reaction kinetics, we investigated the impact of the different ligands on catalytic activity.

A. Different substituents on phosphorous atom

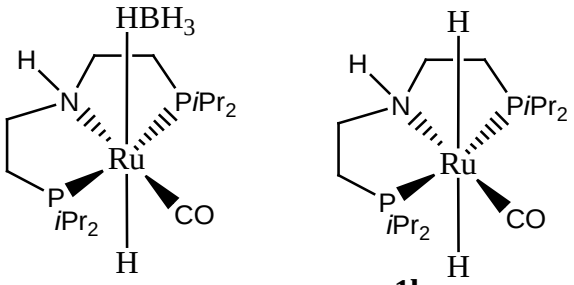

Figure 18. In situ *formed catalysts tested for 1-butanol dehydrogenative coupling.*

These two *in situ* formed catalysts are different from the previously described Ru-MACHO-BH because of their substituent on the phosphorous-PNP atoms (isopropyl instead of phenyl groups).

Both of them were tested into Schlenk tubes, due to their easier deactivation by external oxygen contaminations. The chosen catalyst concentration was around 100 ppm, a value which ensures a linear kinetic regime, not influenced by hydrogen diffusion.

1. Catalytic activity of catalyst **1a**

entry	**m tot cat (g)**	**m tot BuOH (g)**	**n tot cat (mol)**	**n tot BuOH (mol)**	**ppm tot cat**	**ID**
S.T.- 1	0,0117	20,5379	2,59792E-05	0,277089854	93,75737229	S.T. - 93 ppm
S.T.- 2	0,0122	20,6987	2,70894E-05	0,279259309	97,00460706	S.T. - 97 ppm

Table 11. Catalytic tests on cat. ***1a****, conducted into a Schlenk tube at around 100 ppm catalyst loading.*

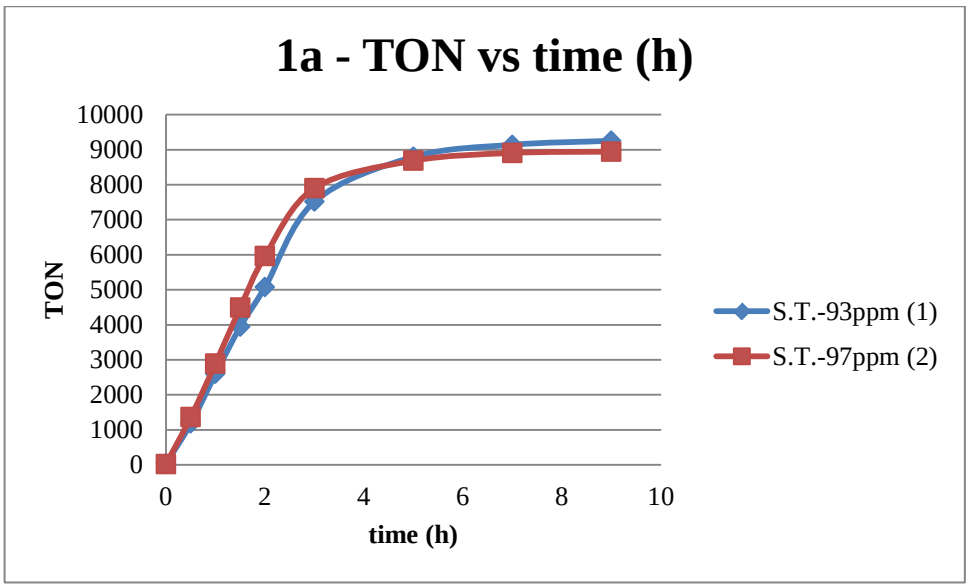

Graphic 14. TON vs time (h). Schlenk tube, 100 ppm catalyst loading.

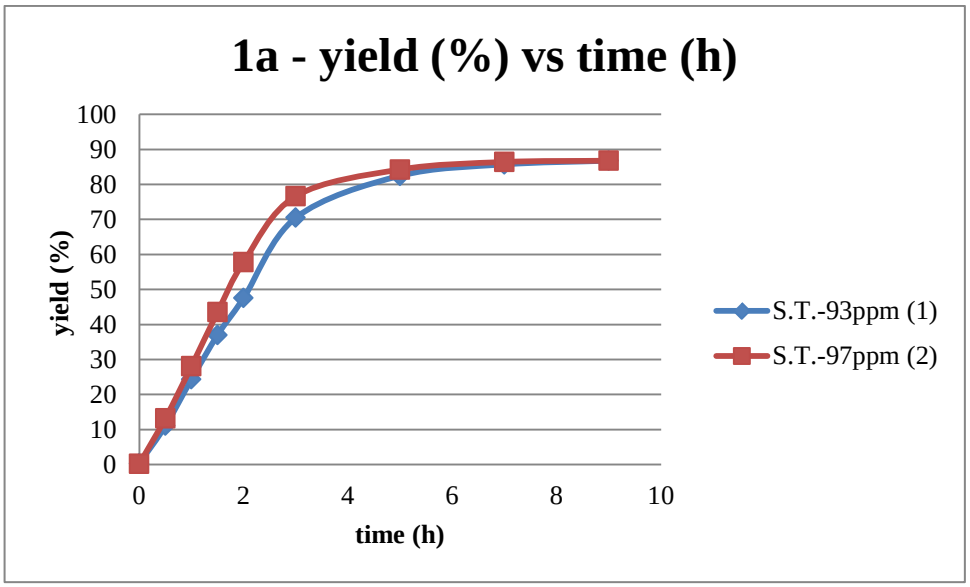

Graphic 15. Yield (%) vs time (h). Schlenk tube, 100 ppm catalyst loading.

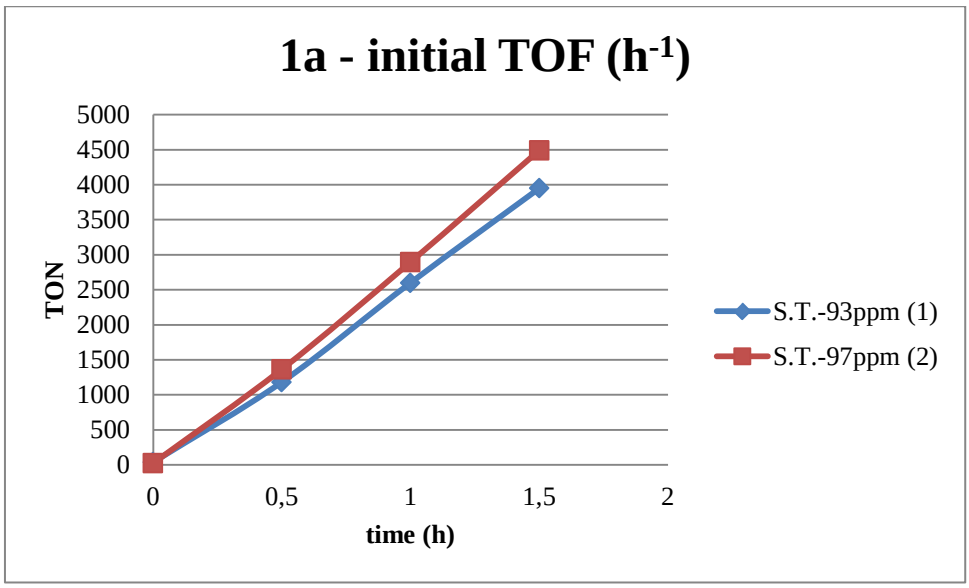

Graphic 16. Initial rate of reactions.

*Table 12. Experimental data for cat. **1a** at 100 ppm catalyst loading.*

entry	max Conversion (%)	max Yield (%)	max TON	initial TOF (h^{-1})
S.T. – 93 ppm (1)	90,1 (after 9 h)	86,8 (after 9 h)	9255 (after 9 h)	2986
S.T. – 97 ppm (2)	88,7 (after 9 h)	86,8 (after 9 h)	8944 (after 9 h)	2630

Catalyst: **1a**; substrate: n-butanol; applied temperature: 130°C; under argon

Preliminary discussions:

Reproducible results were obtained (see Graphic 14 and 15). Catalytic activity seems not strongly influenced by the isopropyl substituent on the phosphorous-PNP atoms. The catalyst can reach good values in terms of TONs, yields, conversions and, TOF_0s (see Table 12).

2. Catalytic activity of catalyst **1b**

entry	m tot cat (g)	m tot BuOH (g)	n tot cat (mol)	n tot BuOH (mol)	ppm tot cat	ID
S.T. - 1	0,0107	20,4668	2,4512E-05	0,276130599	88,7697703	S.T. - 88ppm
S.T. - 2	0,011	20,5059	2,51993E-05	0,276658122	91,08463328	S.T. - 91ppm
S.T. - 3	0,0108	20,528	2,47411E-05	0,276956287	89,3322722	S.T. - 89ppm

*Table 13. Catalytic tests on cat. **1b**, conducted into a Schlenk tube at around 100 ppm catalyst loading*

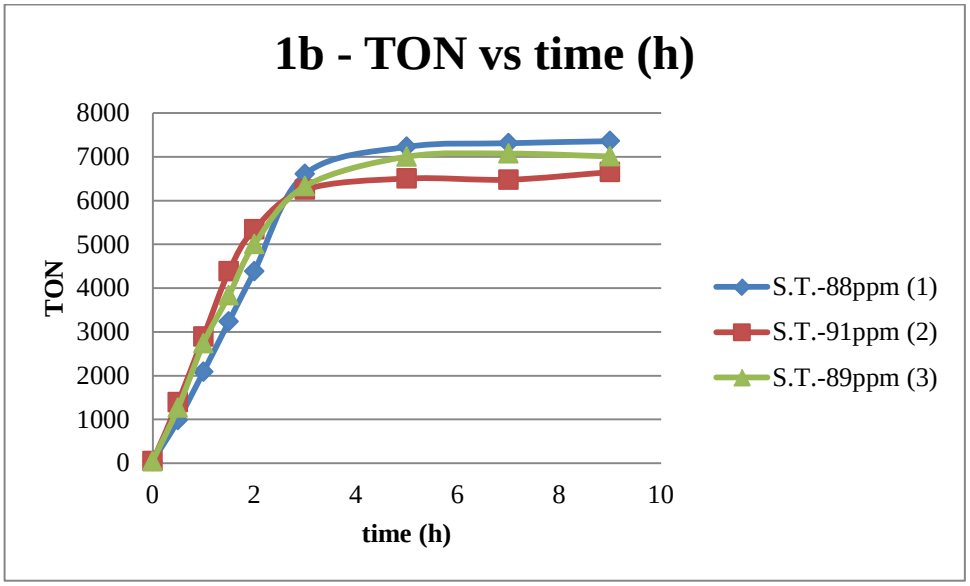

Graphic 17. TON vs time (h). Schlenk tube, 100 ppm catalyst loading.

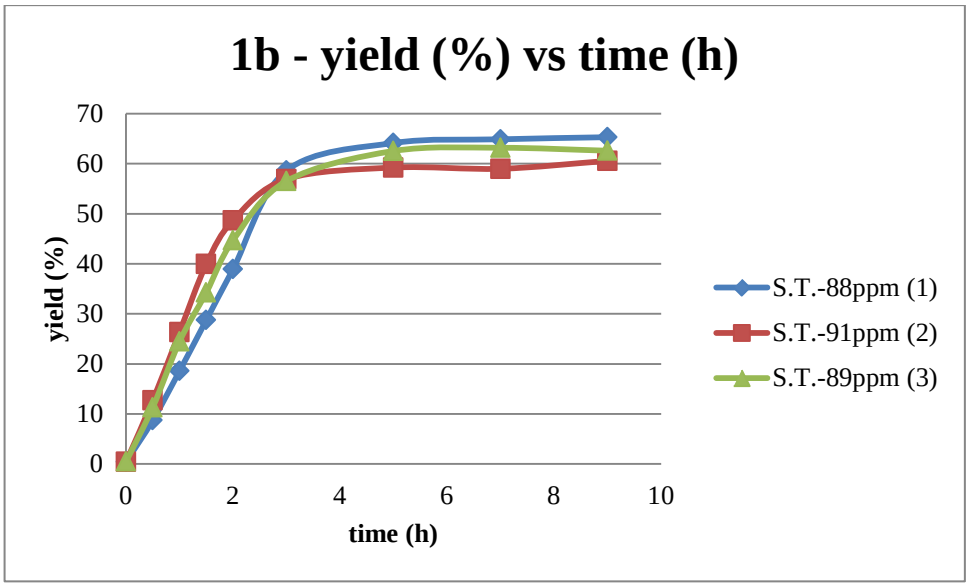

Graphic 18. Yield (%) vs time (h). Schlenk tube, 100 ppm catalyst loading.

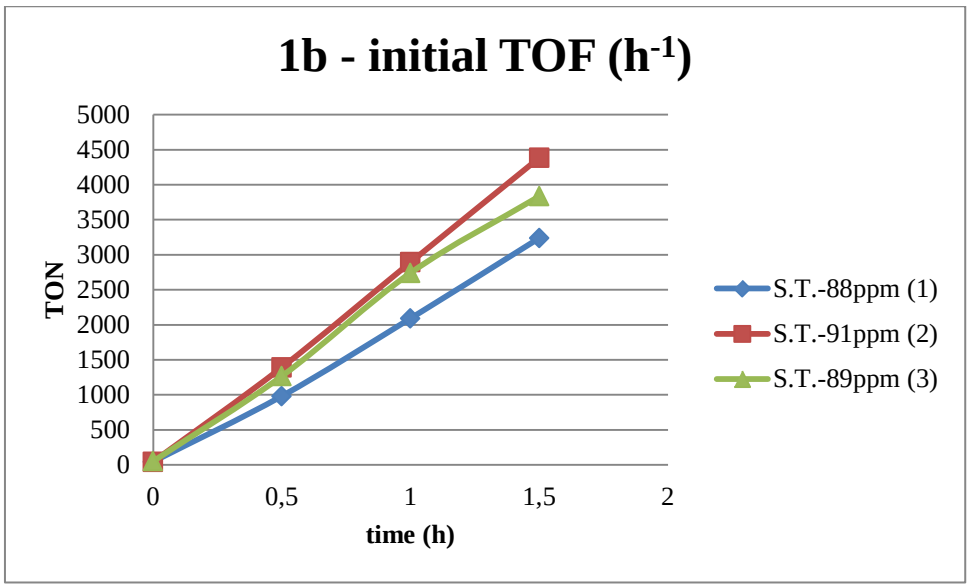

Graphic 19. Initial rate of reactions.

Table 14. Experimental data for cat. ***1b*** *at 100ppm catalyst loading.*

entry	max Conversion (%)	max Yield (%)	max TON	initial TOF (h^{-1})
S.T. – 88ppm (1)	67,2 (after 9 h)	65,3 (after 9 h)	7357 (after 9 h)	2137
S.T. – 91ppm (2)	62,8 (after 9 h)	60,6 (after 9 h)	6650 (after 9 h)	2903
S.T. – 89ppm (3)	64,3 (after 9 h)	63,2 (after 7 h)	7074 (after 7 h)	2565

Catalyst: **1b**; substrate: n-butanol; applied temperature: 130 °C; under argon.

Preliminary discussions:

Reproducible results were obtained (see Graphic 17 and 18). The catalyst cannot reach high values of yields, conversions, and TONs, maybe because of its easier deactivation (two hydride substituents in the *trans* position are very sensitive to external oxygen contaminations and can be very easily released).

3. Comparison and discussions

The following graphs are referred to the best experimental data resulting from catalytic tests on the three complexes seen so far (see entry 3 Table 6, entry 2 Table 12, entry 1 Table 14).

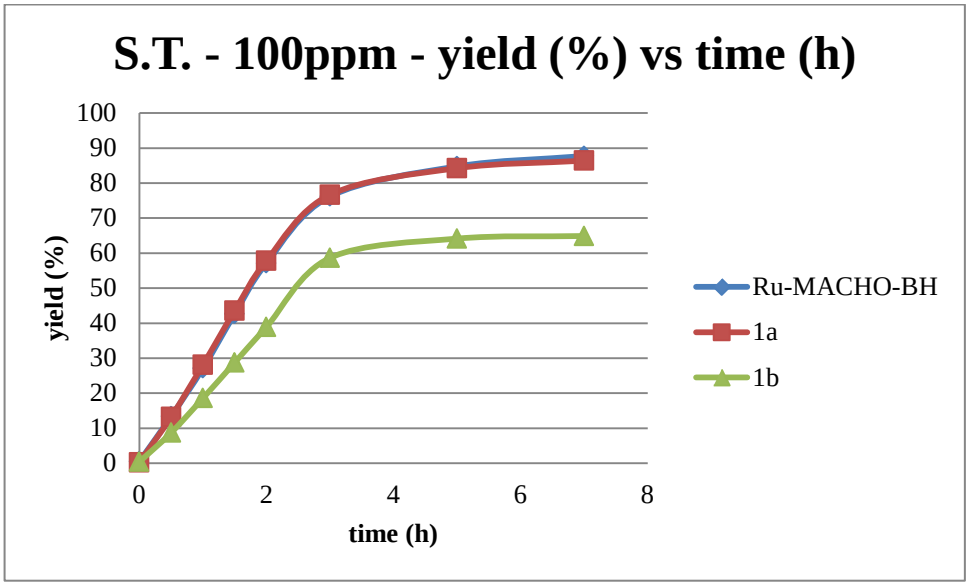

Graphic 20. Comparison between different catalysts: yield (%).

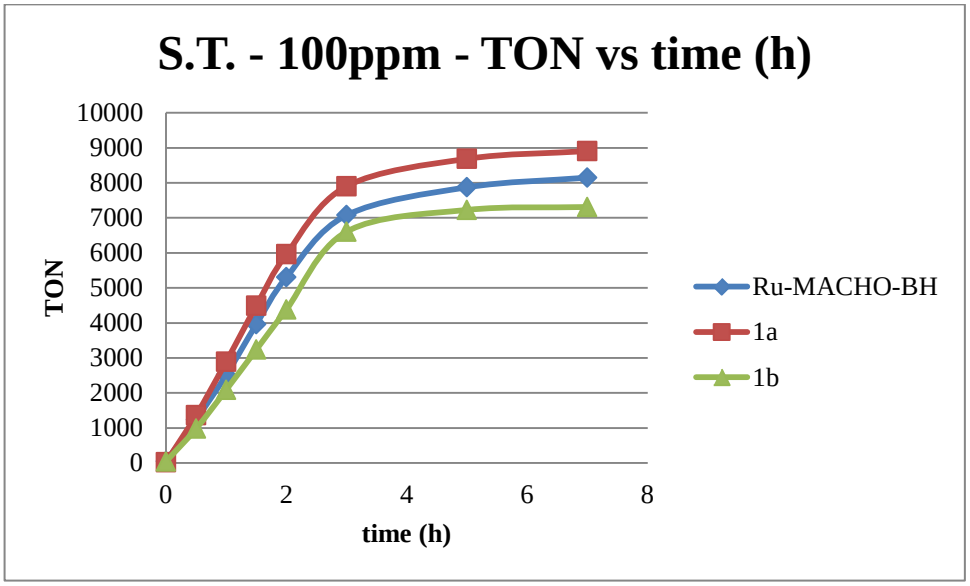

Graphic 21. Comparison between different catalysts: TON.

As shown in the graphs, a change of the phosphorous-PNP substituent from biphenyl to diisopropyl groups did not strongly influenced catalytic activities (see Graphic 20). Also for catalyst **1b**, which shows the worst values of conversion and yields, the progress of the reaction seemed almost similar to the ones recorded in the other two cases (see Graphic 21).

B. Different ligands on ruthenium metal center

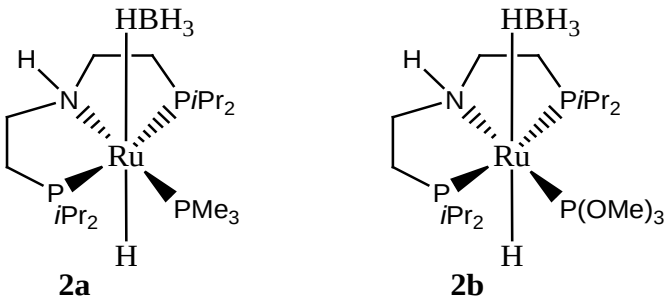

2a **2b**

Figure 19. In situ *formed catalysts for 1-butanol dehydrogenative coupling.*

These two *in situ* formed catalysts differ from the others because of the ligand in the *trans* position relative to nitrogen (phosphine or phosphite instead of carbon oxide).

Whereas catalyst **2a** is able to catalyze the dehydrogenative coupling of butanol, catalyst **2b** shows no catalytic activity at all. Therefore, below are reported only the experimental data concerning catalyst **2a**.

entry	m tot cat (g)	m tot BuOH (g)	n tot cat (mol)	n tot BuOH (mol)	ppm tot cat	ID
S.T. - 1	0,0124	20,4656	2,48781E-05	0,276114409	90,10075705	S.T. - 90ppm
S.T. - 2	0,0128	20,4863	2,56806E-05	0,276393686	92,91325565	S.T. - 93ppm
T.R. - 1	0,015	20,8681	3,00945E-05	0,281544792	106,8906176	T.R. - 107ppm
T.R. - 2	0,0137	20,2596	2,74863E-05	0,273335132	100,558998	T.R. - 100ppm
T.R - 3	0,0132	20,4756	2,64832E-05	0,276249325	95,86686618	T.R. - 96ppm

*Table 15. Catalytic tests conducted on catalyst **2a** into different reactors at around 100ppm catalyst loading.*

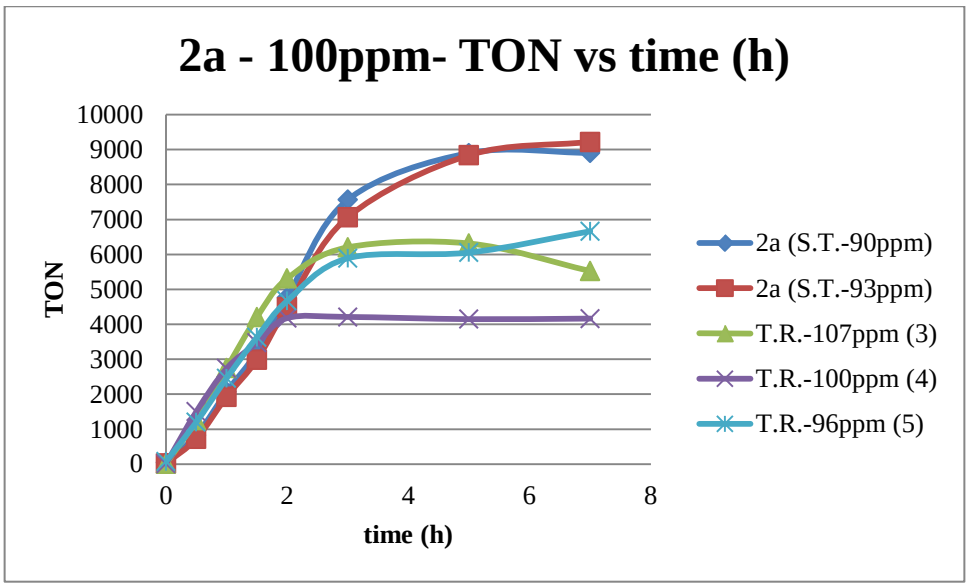

Graphic 22. TON vs time (h). Different reactors, 100ppm catalyst loading.

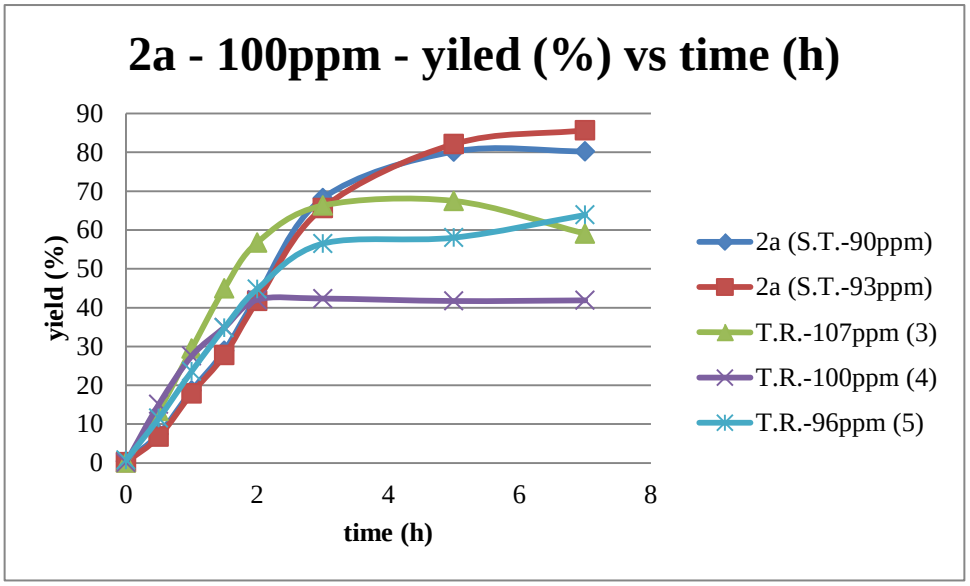

Graphic 23. Yield (%) vs time (h), different reactors, 100ppm catalyst loading.

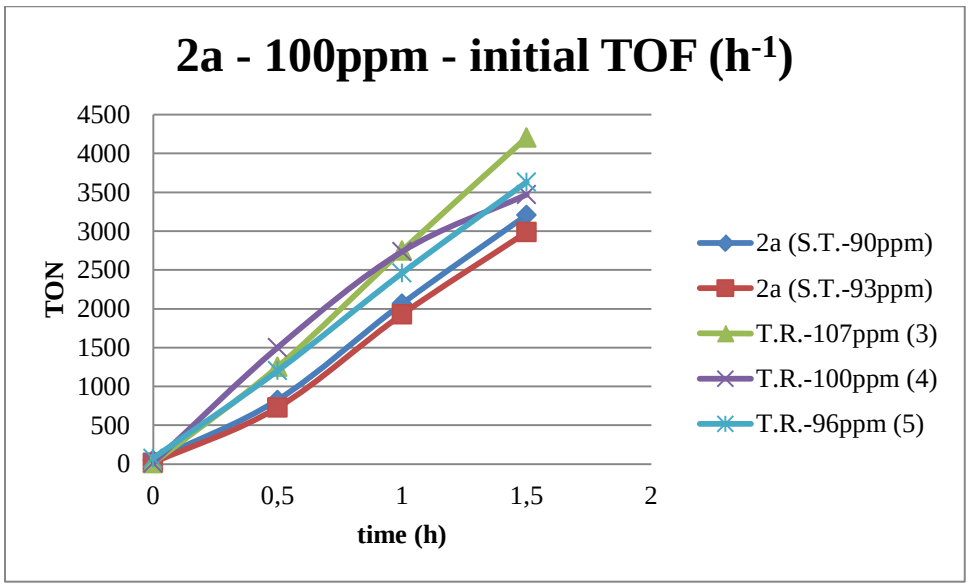

Graphic 24. Initial rate of reactions.

*Table 16. Experimental data for catalyst **2a** at 100ppm catalyst loading.*

entry	max Conversion (%)	max Yield (%)	max TON	initial TOF (h^{-1})
S.T. – 90ppm (1)	83,3 (after 7 h)	80,2 (after 7 h)	8905 (after 7 h)	2143
S.T. – 93ppm (2)	88,1 (after 7 h)	85,7 (after 7 h)	9223 (after 7 h)	2143
T.R. – 107ppm (3)	71,0 (after 5 h)	67,5 (after 5 h)	6313 (after 5 h)	2816
T.R. – 100ppm (4)	47,6 (after 3 h)	42,3 (after 3 h)	4211 (after 3 h)	2322
T.R. – 96ppm (5)	66,9 (after 7 h)	63,9 (after 7 h)	6664 (after 7 h)	2386

Catalyst: **2a**; substrate: n-butanol; applied temperature: 130°C; under argon

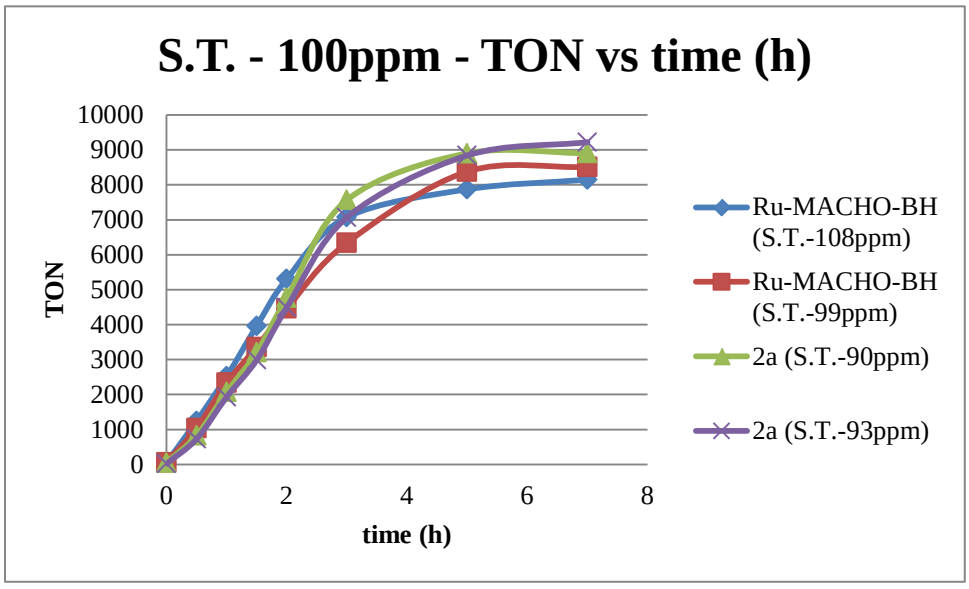

*Graphic 25. Comparison between **Ru-MACHO-BH** and cat. **2a**: TON vs time (h).*

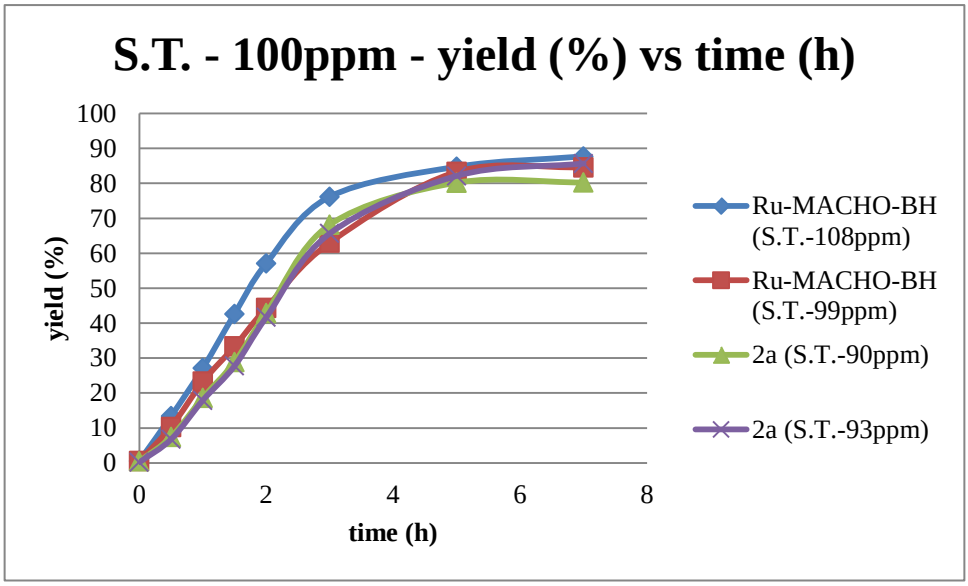

*Graphic 26. Comparison between **Ru-MACHO-BH** and cat. **2a**: yield (%) vs time (h).*

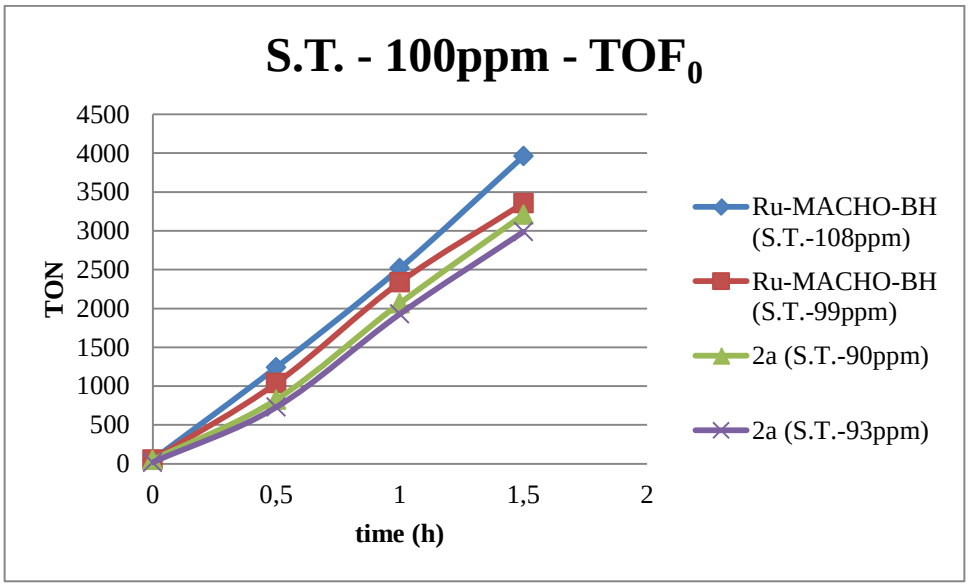

*Graphic 27. Comparison between initial reaction rates for **Ru-MACHO-BH** and cat. **2a**.*

Discussions:

Reproducible results were obtained only when Schlenk tubes were used as reactors (see Graphic 22 and 23). This probably means that the catalyst is strongly influenced by external oxygen contaminations. Reactions seem to have an initial linear kinetic trend that is interrupted after around 2 hours (see Graphic 22, 23 and 24). A comparison of the two catalysts into the same reactor (Schlenk tube) shows that they have similar catalytic activities and initial reaction rates (see Graphic 25, 26 and 27). This fact confirms that, at 100 ppm catalyst loading, proper reaction kinetics are ensured.

The CO ligand in the *trans* position relative to the nitrogen-PNP atom in Ru-MACHO-BH guarantees a more stable complex, i.e. less oxygen sensitive. Its replacement with a phosphine ligand PMe_3 does not seem to have a too strong influence on the catalytic activity of the complex.

Additional studies are needed to explain the complete inactivity of the complex **2b** bearing a phosphite $P(OMe)_3$ ligand instead of the CO (or PMe_3). Hypotheses on this regard could concern the more electron-attracting nature of the phosphite group, in comparison to those of CO and PMe_3: this may lower the electron-density on the ruthenium center, making the catalytic cycle unfeasible. Another reason that could affect the reactivity of the whole complex might be linked to the slightly increased bulkiness of the phosphite moiety, which could bring about a higher steric hindrance. In any case, the nature of the binder in the *trans* position relative to the NH group of PNP ligand do seem to influence the catalytic activity of the complex in the dehydrogenative coupling of butanol, indicating that this ligand is involved in the catalytic cycle (directly or by providing assistance to other ligands).

4.3. Catalyst deactivation/reactivation

At the end of the reaction, the catalyst is transformed into a deactivated species. Mass Spectrometry studies conducted on the deactivated catalyst showed that activation or inhibition of the catalyst active site is related to the moiety that is "on the top" of the complex, i.e. opposite to the ruthenium-hydride bond. Unfortunately, it was not possible to get information about the nature of the moiety that brings about catalyst deactivation since the only molecular ion observed by MS analysis is the complex with the "top" position free.

Even the ^1H NMR spectrum of the deactivated catalyst did not provide any clear information.

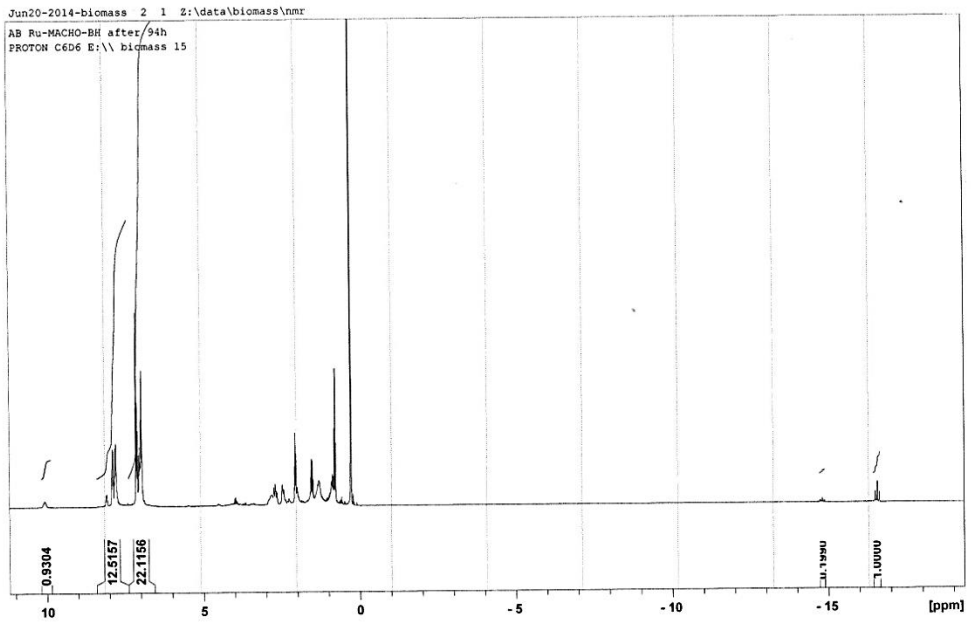

*Figure 20. ^{1}H NMR of deactivated **Ru-MACHO-BH** after 94 hours reaction.*

However, studies have been conducted on the possibility of reactivation of the catalyst after the exhaustion of its activity. Two routes were followed:

- catalyst reactivation by base-addition;
- catalyst reactivation by temperature increase.

Various experiments were performed to make a proper comparison of the results. First, the reaction was performed at 90 °C and, when the catalyst exhausted its activity, the temperature was increased at 130 °C. Then, another reaction was carried out at 90 °C until completion. The catalyst derived from this very long reaction was then recovered and used to perform other two reactions: the first one with an additional base (1.3% EtONa), the second one at a higher temperature (130 °C). All reactions were conducted into Schlenk tubes, using **Ru-MACHO-BH** as catalyst, at 500 ppm catalyst concentration, and with n-butanol as substrate.

Table 17. Catalytic tests conducted on Ru-MACHO-BH (500ppm) under different conditions.

entry	m cat (g)	m BuOH (g)	m EtONa (g)	n cat (mol)	n BuOH (mol)	n EtONa (mol)	ppm cat	ID
1	0,0639	16,0178	///	0,00010899	0,2161063	///	504,3543	504ppm (90-130°C)
2	0,0651	16,235	///	0,000111	0,2190367	///	506,95153	507ppm (90°C)
3	0,0255	6,15	///	4,34953E-05	0,082973556	///	524,20699	524ppm (residual) 130°C
4	0,0268	6,157	0,0858	4,57127E-05	0,083067998	0,001261	550,3049	550ppm (residual) EtONa 90°C

Catalyst: **Ru-MACHO-BH**; reactor: Schlenk tube; substrate: n-butanol; applied temperature: 90°C (entry 1, 2 and 4), 130°C (entry 3 from beginning, and 1 after 47 hours); under argon

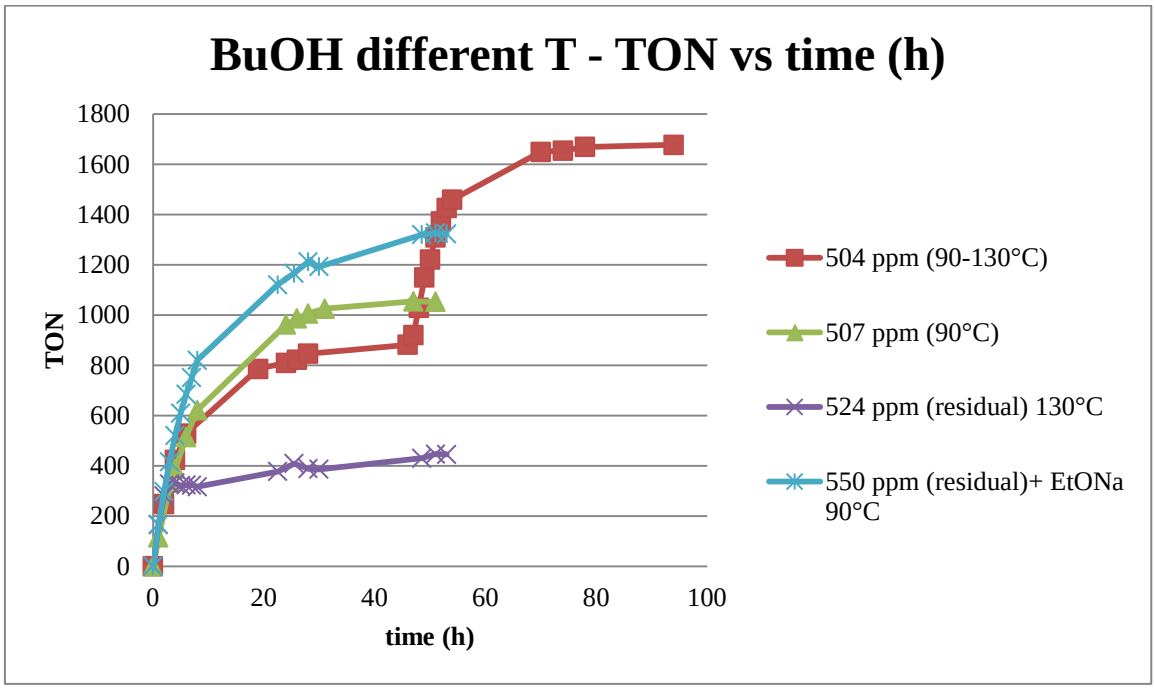

Graphic 28. Comparison between different conditions of Ru-MACHO-BH deactivation: TON vs time (h).

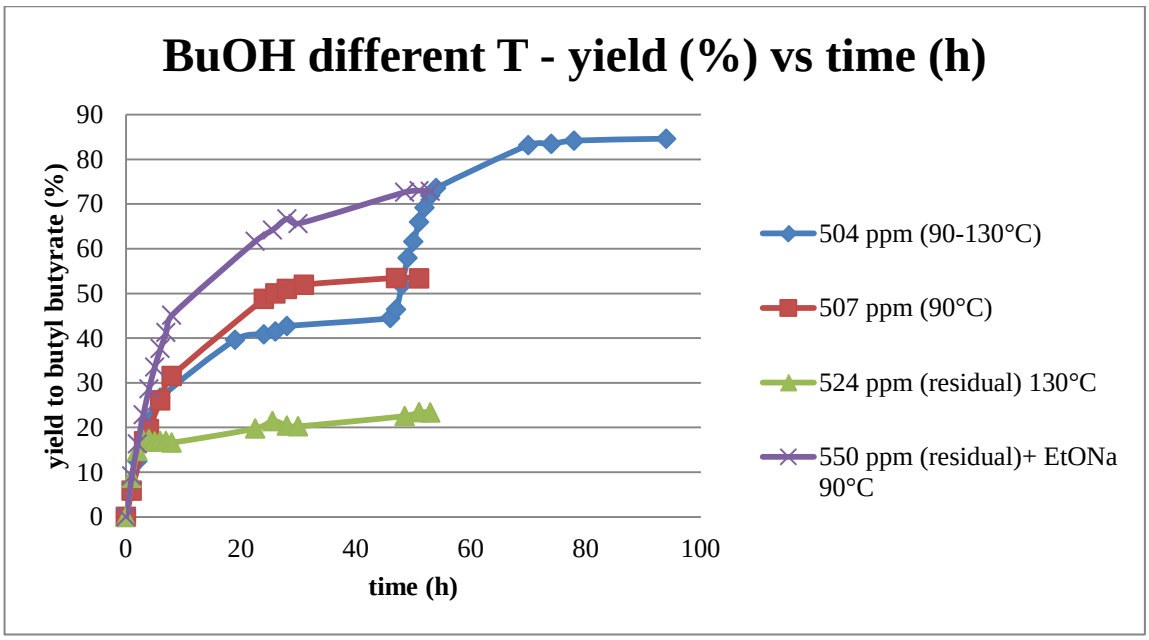

Graphic 29. Comparison between different conditions of Ru-MACHO-BH deactivation: yield (%) vs time (h).

504 ppm (90 - 130°C)			507 ppm (90°C)		
time (h)	**Yield (%)**	**TON**	**time (h)**	**Yield (%)**	**TON**
0	0	0	0	0	0
2	12,468	114392,8	1	5,868	52845,7
4	21,355	195932,1	3,2	16,915	152330,2
6	26,642	244440,2	4	19,662	177071,6
19	39,638	363675,9	6	26,077	234841
24	40,864	374918,4	8	31,508	283755,3
26	41,495	380713,6	24	48,785	439344,5
28	42,676	391542,4	26	50,022	450475,6
46	44,488	408168,7	28	50,993	459227,6
47	46,398	425696,2	31	51,975	468070,8
48	51,886	476045,1	47	53,465	481497,2
49	57,976	531919,7	51	53,373	480661,9
50	61,580	564986,6			
51	65,996	605498,6			
52	69,240	635265,1			
53	71,919	659845,2			
54	73,591	675189,8			
70	83,194	763295,9			
74	83,441	765556,9			
78	84,199	772518,6			
94	84,623	776408,3			

550 ppm (residual) + 1,26 % EtONa			524 ppm (residual) 130°C		
time (h)	**Yield (%)**	**TON**	**time (h)**	**Yield (%)**	**TON**
0	0	0	0	0	0
1	9,163	200446,3	1	8,737	200892,5
2	16,339	357421,3	2	14,756	339267,6
3	22,855	499968,3	3	17,208	395635,1
4	28,664	627051,0	4	17,385	399710,5
5	33,561	734167,2	5	16,860	387643,7
6	37,689	824468,2	6	16,977	390332,1
7	41,297	903409,7	7	16,957	389865,5
8	45,137	987411,8	8	16,624	382220,7
22,5	61,673	1349139,1	22,5	19,769	454532,2
25,5	64,205	1404533,9	25,5	21,458	493345,8
28	66,687	1458812	28	20,393	468876,9
30	65,647	1436067,4	30	20,260	465813,3
48,5	72,648	1589220,1	48,5	22,564	518776,7
51	72,987	1596643,7	51	23,411	538264,2
53	72,827	1593155,3	53	23,357	537025,8

Table 18. Experimental data relative to Ru-MACHO-BH deactivation/reactivation.

entry	**ID**	**TOF_0 (h^{-1})**	**TOF 130°C (h^{-1})**
1	504ppm (90-130°C)	88,048	77,592
2	507ppm (90°C)	97,649	///
3	524ppm (residual) 130°C	109,963	///
4	550ppm (residual) 1,26% EtONa	137,634	///

Table 19. Different reaction rates for catalyst reactivation.

Discussions:

Reactivation of the catalyst seems to be possible in both cases. The temperature certainly affects catalytic activity since, at 90 °C, the reaction cannot reach high values of yield and TON, even for high catalyst concentration (more than 500 ppm) and very long reaction time (maximum yield = 72,8% after 53 hours, lower than that obtained after 5 hours at 130 °C with half of catalyst loading, see Graphic 1 and 2). The *in situ* increase of the temperature provides the best values of catalytic activity and productivity, indicating that transformation of the catalyst into a deactivated species can be reversed by a temperature increase (see Graphic 28 and 29). This aspect seems to be confirmed by the TOFs. Comparable values were indeed obtained at 90 °C and 130 °C (see entry 1, Table 19): this

would suggest catalyst reactivation and a concomitant, effective restart of the dehydrogenative coupling.

Also the catalyst recovered after 53 hours seems to be reactivated by both methods, but in this case, the stronger effect derives from the addition of 1,26 mol% of EtONa without increasing the temperature (see entry 3 and 4, Table 19, and Graphics 28 and 29). Further analysis are needed to give a full explanation of this aspects, involving complete characterization of the catalyst at the end of the catalytic cycle.

5- Conclusions

Acceptorless dehydrogenative coupling (ADC) of alcohols is a green, atom-efficient route to produce useful, versatile symmetrical esters, conveniently accompanied by formation of hydrogen gas. Application of this reaction to the widely available products arising from biomass has captured great attention in recent times.

A new generation of homogeneous pincer catalysts has proved to be particularly suitable for this type of transformation, especially those bearing a tridentate PNP ligand bonded to the ruthenium metal center. However, the described oxygen-sensitive complexes, although very active, did not appear to have good productivities, and, in most reported cases, required an additional base or solvent. The most challenging substrates for this type of reaction are short chain primary alcohols, such as building blocks deriving from biomass: ethanol and butanol.

In the present work, the catalytic performances of both isolated and *in situ* formed Ru-PNP complexes have been investigated for both the base and the solvent-free transformation of 1-butanol into butyl butyrate, a symmetrical ester largely used in flavor industries. An overview of the influence of reactor type and reaction conditions, such as temperature, catalyst concentration and structure, has been possible through a comparison between the different catalytic systems.

The results can be summarized as follows:

- a detailed study on the reactors has revealed the importance of an effective system for the disposal of the released hydrogen, which influences reaction kinetics. In this regard, the best system has proved to be a Schlenk tube equipped with mechanical stirrer and baffles, which guarantees the best values of initial reaction rate and the highest yields and conversions. For the treatment of higher volumes of reactant the problem of contamination by external oxygen can be a crucial point, since this could lead to catalyst deactivation. This problem is more noticeable when treating low catalyst concentrations, therefore for long reaction times;

- catalytic tests have been carried out to find the right catalyst loading ensuring both proper reaction kinetics, and minor contamination problems. Those tests, performed on the commercial catalyst Ru-MACHO-BH, have proved that at 250 ppm kinetics is strongly influenced by hydrogen diffusion, while at 20 or 60 ppm the reaction

time is too long and oxygen contamination problems lead to a decrease in general productivity. An intermediate catalyst concentration of 100 ppm can eliminate both problems, guaranteeing optimal catalytic performance with yields and conversions higher than 90%, TONs of more than 8000 and initial rates up to 4500 h^{-1}.

- *in situ* catalysts have been synthesized to better understand the role of the different ligands on the catalytic activity and to find a new catalyst with performances comparable to those of the very expensive **Ru-MACHO-BH**. The nature of the substituent on the phosphorous atom of the PNP binder did not seem to have a significant influence on catalytic activity, while modifying the ligand on the top of the complex (*trans* position to hydride) or the one in the *trans* position relative to the PNP-NH group, strongly influences catalytic performances. HBH_3 has proved to be a stronger ligand than hydride, conferring less oxygen sensitivity and more selectivity to the complex. The best catalysts analyzed are the very ones with a borohydride binder on the head of the complex (**Ru-MACHO-BH**, **1a**, **2a**). Changing the CO ligand with the phosphine $P(CH_3)_3$ leads to a decrease of the catalytic performances, probably due to an increased oxygen sensitivity. In fact catalyst **2a** can reach high values of yields and conversions (more than 85 %), TONs up to 9000 and initial TOF of more than 2000 h^{-1}, nevertheless worse than **Ru-MACHO-BH**. Further studies are needed to better understand the role of the ligands involved in the catalytic cycle;

- temperature has an influence on the catalytic activity. At 90 °C the catalyst shows less activity and lower reaction rate than at 130 °C. This fact is not simply due to the higher boiling point of butanol (118 °C), which does not allow to work under reflux conditions, since parallel studies conducted on ethanol (b.p. = 78 °C) have evidenced the same problem. Also in this case additional studies are required;

- temperature has also an influence on catalyst reactivation: an increase in the temperature from 90 °C to 130 °C leads to catalyst reactivation. A hypothetical explanation could entail transformation of the active catalyst into a deactivated species by exchange of the ligand "on the top" of the complex with some other moiety: the latter can be subsequently released with concomitant catalyst reactivation. This release is made possible both/either by an increase of the temperature and/or by an addition of a base. In fact, the best results in terms of catalyst reactivation are obtained in presence of 1.26 mol% of EtONa. However, it

is worth pointing out that, as previously explained, addition of a base should be avoided to ensure an environmentally friendly process.

Although further studies are certainly necessary to thoroughly understand the reaction behaviour, the catalytic performances of the developed catalysts can be definitely considered better than those so far described in literature.

References

[1] REN21, Renewables 2013 Global Status Report, http://www.ren21.net/REN21Activities/GlobalStatusReport.aspx .

[2] *"Internal Documents: BP Estimates Oil Spill Rate up to 100,000 Barrels Per Day"*. Consumer Energy Report. *Retrieved 20 June 2010.*

[3] http://ec.europa.eu/programmes/horizon2020/ .

[4] http://www.bbi-europe.eu .

[5] US Patent 1 315 585.

[6] O.I. Shapovalov, L.A. Ashkinazi, *Russian J. Of Apll. Chem*., **2008**, *81* , pp. 2232-2236.

[7] N. T. Dunford. *Food and Industrial Bioproducts and Bioprocessing*, **2012**, Wiley. p. 195.ISBN 9781119946052.

[8] T. C. Ezeji, N. Qureshi, H. P. Blaschek, "Butanol fermentation research: Upstream and downstream manipulations*" Chem. Rec.* **2004**, *4*, 305–314.

[9] J. H. Clark "Green Chemistry for the second generation biorefinery – sustainable chemical manufacturing based on biomass" *J. of Chem., Tech. and Biotech.*, **2007**, *82*, pp.603-609.

[10] P. M. Schenk, S. R. Thomas-Hall, E. Stephens, U. C. Marx, J. H. Mussgnug, C. Posten, O. Kruse, B. Hankamer "Second generation Biofuels: High-Efficiency Microalgae for Biodiesel Production" *Bioenerg. Res.*, **2008,** *1*, 20–43.

[11] R, C. Brown, *Biorenewable Resources Engineering New Products from Agriculture*. Iowa State Press, **2003,** Ames IA.

[12] D. M. Teegarden, *Polymer Chemistry: Introduction to an Indispensable Science*, NTSA Press, National Science Teachers Association, **2004**.

[13] J. I. Qazi, N. Chaudhary, S. S. Mirza, in *Biofuel Production-Recent Developments and Prospects*, **2011**, pp.247-292

[14] J. Shokri, K. Adibkia, in *Cellulose – Medical, Pharmaceutical and Electronic Applications*, **2013**, pp. 47-66.

[15] F. D. Marques-Marinho, C. D. Vianna-Soares, in *Cellulose – Medical, Pharmaceutical and Electronic Applications*, **2013**, pp. 141-162.

[16] A. Baptista, I. Ferreira, J. Borges, in *Cellulose – Medical, Pharmaceutical and Electronic Applications*, **2013**, pp. 1-18.

[17] S. Wang, Y. Yu, in *Cellulose – Medical, Pharmaceutical and Electronic Applications*, **2013**, pp. 195-214.

[18] J. M. Moran-Mirabal, in *Cellulose – Fundamental Aspects*, **2013**, pp.1-44.

[19] E. M. Rubin, *Nature*, **2008**, *454*, 841-845.

[20] M. Ni, D. Y. C. Leung, K. Sumathy, *Fuel Process. Technol.* **2006**, 87, 461-472.

[21] K. Nakashima, K. Yaniguchi, S. Arai, R. Yamada, S. Katahira, N. Ishida, H. Takahashi, C. Ogino, A. Kondo, *Green Chem*. **2011**, *13*, 2948-2953.

[22] Hemp Body Car, patent 2.269.452 (13/02/42).

[23] G. Jurgens, S. Survase, O. Berezina, E. Sklavounos, J. Linnekoski, A. Kurkijarvi, M. Vakeva, A. van Heiningen, T. Granstrom, *Biotechnol. Lett* **2012**, *34*, 1415-1434.

[24] T. Ezeji, N. Qureshi, H. P. Blaschek "Butanol Production From Agricultural Residues: Impact of Degradation Products on Clostridium beijerinckii Growth and Butanol Fermentation" *Biotechnology and Bioengineering*, **2007**, *97*, 6.

[25] K. P. Michael, N. Steffi, D. R. Peter, in *Biofuel Production-Recent Developments and Prospects*, **2011**, pp.451-468.

[26] K. Yamaguchi, K. Mori, T. Mizugaki, K. Ebitani, K. Kaneda, *J. Am. Chem. Soc.* **2000**, *122*, 7144-7145.

[27] M. S. Sigman, D. R. Jensen, *Acc. Chem. Res.* **2006**, *39*, 221-229.

[28] C. Gunanathan, D. Milstein, *Science*, **2013**, *341*.

[29] M. H. S. A. Hamid, P. A. Slatford, J. M. J. Williams, *Adv. Synth. Catal.* **2007**, *349*, 1555-1575.

[30] D. Morton, D. J. Cole-Hamilton, *J. Chem. Soc., Chem. Commun.*, **1987**, 248-49.

[31] D. Morton, D. J. Cole-Hamilton, I. D. Utuk, M. Paneque-Sosa, M. Lopez-Poveda, *J. Chem. Soc., Dalton Trans*, **1989**, 489-495.

[32] D. Morton, D. J. Cole-Hamilton, *J. Chem. Soc., Chem. Commun.*, **1988**, 1154-1156.

[33] L.-C. Yang, T. Ishida, T. Yamakawa, S. Shinoda, *J. Mol. Catal. A:Chem*. **1996**, *108*, 87-93.

[34] Y. Takano, M. A. Herranz, N. Martìn, S. G. Radhakrishnan, D. M. Guldi, T. Tsuchiya, S. Nagase, T. Akasaka, *J. Am. Chem. Soc.*, **2010**, *132*, 8048-8055.

[35] A. Dobson, S. D. Robinson, *Inorg. Chem*., **1977**, *16*, 137-142.

[36] A. Dobson, S. D. Robinson, *J. Organomet. Chem.*, **1975**, *87*, C52-C53.

[37] N. Sieffert, R. Réocreux, P. Lorusso, D. J. Col-Hamilton, M. Buhl, *Chem. Eur. J.*, **2014**, *20*, 4141-4155.

[38] C. W. Yung, P. E. Garrou, *Organometallics*, **1982**, *1*, 658-666.

[39] C. Gunanathan, D. Milstein, *Acc. Chem. Res.*, **2011**, *44*, 588-602.

[40] D. Milstein, *Top Catal*., **2010**, *53*, 915-923.

[41] C. Gunanathan, D. Milstein, in *Bifunctional Mulecular Catalysis*, Vol. 37 (Eds.:T. Ikariya, M. Shibasaki), Springer Berlin Heidelberg, **2011**, pp.55-84.

[42] J. Zhang, M. Gandelman, L. J. W. Shimon, H. Rozenberg, D. Milstein, *Organometallics*, **2004**, *23*, 4026-4033.

[43] M. Nielstein, A. Kammer, D. Cozzula, H. Junge, S. Gladiali, M. Beller, *Angew. Chem. Int. Ed*., **2011**, *50*, 9593-9597.

[44] Y. Blum, D. Reshef, Y. Shvo, *Tetrahedron Lett.***1981**, *22*, 1541-1544.

[45] Y. Blum, Y. Shvo, *J. Organomet. Chem*., **1984**, *263*, 93-107.

[46] Y. Blum, Y. Shvo, *J. Organomet. Chem*., **1985**, *282*, C7-C10.

[47] S. Murahashi, T. Naota, K. Ito, Y. Maeda, H. Taki, *J. Org. Chem.* **1987**, *52*, 4319-4327.

[48] J. Zhang, G. Leitus, Y. Ben-Davis, D. Milstein, *J. Am. Chem. Soc*., **2005**, *127*, 10840-10841.

[49] J. Zhang, M. Gandelman, L. J. W. Shimon, D. Milstein, *Dalton Trans*. **2007**, 107-113.

[50] J. Zhang, E. Balaraman, G. Leitus, D. Milstein, *Organometallics*, **2011**, *30*, 5716-5724.

[51] D. Spasyuk, D. G. Gusev, *Organometallics*, **2012**, *31*, 5239-5242.

[52] M. Bertoli, A. Choualeb, A. J. Lough, B. Moore, D. Spasyuk, D. G. Gusev, *Organometallics*, **2011**, *30*, 3479-3482.

[53] D. Spasyuk, S. Smith, D. G. Gusev, *Angew. Chem. Int. Ed*., **2012**, *51*, 2772-2775.

[54] M. Bertoli, A. Choualeb, D. G. Gusev, A. J. Lough, Q. Major, B. Moore, *Dalton Trans*., **2011**, *40*, 8941-8949.

[55] A. Friedrich, M. Drees, J. Schmedt auf der Guaanne, S. Schneider, *J. Am. Chem. Soc*., **2009**, *131*, 17552-17553.

[56] M. Nielstein, H. Junge, A. Kammer, M. Beller, *Angew. Chem. Int. Ed*., **2012**, *51*, 5711-5713.

[57] D. Bradley, G. Williams, M. Lawton, *J. Org. Chem.* **2010**, *75*, 8351-8354.

[58] M. Kass, A. Friedrich, M. Drees, S. Schneider, *Angew. Chem. Int. Ed*., **2009**, *48*, 905-907.

[59] N. Ahmad, J. J. Levison, S. D. Robinson, M. F. Uttley, *Inorg. Synth*., **1974**, *15*, 45-64.

[60] M. Bertoli, A. Choualeb, A. J. Lough, D. Spasyuk, D. G. Gusev, *Organometallics*, **2011**, *30*, 3479-3482.

[61] D. Spasyuk, S. Smith, D. G. Gusev, *Angew. Chem. Int. Ed.*, **2013**, *52*, 2538-2542.

[62] *"Procédé de synthèse d'esters et catalyseur de ladite synthèse", **08.11.2013**, N° 1360981*

[63] M. Nielstein, E. Alberico, W. Baumann, H. J. Drexler, H. Junge, S. Gladiali, M. Beller, *Nature*, **2013**, *495*, 85-89